

# Phosphatidic acid phospholipase A1 mediates ER–Golgi transit of a family of G protein–coupled receptors

Govind Kunduri,<sup>1</sup> Changqing Yuan,<sup>1</sup> Velayoudame Parthibane,<sup>1</sup> Katherine M. Nyswaner,<sup>1</sup> Ritu Kanwar,<sup>1</sup> Kunio Nagashima,<sup>2</sup> Steven G. Britt,<sup>3</sup> Nickita Mehta,<sup>4</sup> Varshika Kotu,<sup>4</sup> Mindy Porterfield,<sup>4</sup> Michael Tiemeyer,<sup>4</sup> Patrick J. Dolph,<sup>5</sup> Usha Acharya,<sup>6</sup> and Jairaj K. Acharya<sup>1</sup>

<sup>1</sup>Laboratory of Cell and Developmental Signaling, National Cancer Institute, Frederick, MD 21702

<sup>2</sup>Electron Microscopy Laboratory, Frederick National Laboratory for Cancer Research, Frederick, MD 21702

<sup>3</sup>Department of Cell and Developmental Biology, University of Colorado, Aurora, CO 80045

<sup>4</sup>Complex Carbohydrate Research Center, The University of Georgia, Athens, GA 30602

<sup>5</sup>Department of Biological Sciences, Dartmouth College, Hanover, NH 03755

<sup>6</sup>Program in Gene Function and Expression, University of Massachusetts Medical School, Worcester, MA 01605

The coat protein II (COPII)-coated vesicular system transports newly synthesized secretory and membrane proteins from the endoplasmic reticulum (ER) to the Golgi complex. Recruitment of cargo into COPII vesicles requires an interaction of COPII proteins either with the cargo molecules directly or with cargo receptors for anterograde trafficking. We show that cytosolic phosphatidic acid phospholipase A1 (PAPLA1) interacts with COPII protein family members and is required for the transport of Rh1 (rhodopsin 1), an N-glycosylated

G protein-coupled receptor (GPCR), from the ER to the Golgi complex. In *papla1* mutants, in the absence of transport to the Golgi, Rh1 is aberrantly glycosylated and is mislocalized. These defects lead to decreased levels of the protein and decreased sensitivity of the photoreceptors to light. Several GPCRs, including other rhodopsins and *Bride of sevenless*, are similarly affected. Our findings show that a cytosolic protein is necessary for transit of selective transmembrane receptor cargo by the COPII coat for anterograde trafficking.

## Introduction

Secretory and membrane proteins are synthesized in the ER and undergo appropriate posttranslational modifications and folding before making their way through the anterograde secretory pathway, including the Golgi complex, to their final destination (Rothman, 1994). While in transit, they undergo further modifications, e.g., trimming or addition of the glycosyl residues on an N-glycosylated protein. The posttranslational modifications bestowed upon any protein is unique to that individual protein and is directed in part by discrete signals that reside in the protein itself, and the alterations are determined by modifying proteins that are segregated in distinct organelles along

the secretory pathway (Barlowe and Miller, 2013). In general, the folding and early posttranslational modifications rendered in the ER ensure the overall functional fitness of many proteins; however, the stability, specificity, and proper localization of a significant fraction of transported proteins is influenced greatly by their fate in the post-ER compartments. An essential task of the cell is to safeguard that each of these proteins is delivered to the correct subcellular location. An important interaction of a newly synthesized secretory/membrane protein is with the coat protein II (COPII) complex that ensures proper packaging into ER-derived membrane vesicles and delivery to the Golgi complex. COPII protein complex consists of five core proteins: Sar1, Sec23, Sec24, Sec13, and Sec31 (Fromme et al., 2008; Zanetti et al., 2012). Activated Sar1 recruits Sec23/Sec24

G. Kunduri and C. Yuan contributed equally to this paper.

Correspondence to Jairaj K. Acharya: acharya@jcbmail.nih.gov

Abbreviations used in this paper: AmBic, ammonium bicarbonate; BAC, bacterial artificial chromosome; COPII, coat protein II; ERG, electroretinogram; GPCR, G protein-coupled receptor; hs, heat shock; MS, mass spectrometry; PAPLA1, phosphatidic acid phospholipase A1; PNGase F, peptide N-glycosidase F; Sec23IP, Sec23-interacting protein; SR-SIM, superresolution structured illumination microscope; Trp, transient receptor potential; UAS, upstream activating sequence.

This article is distributed under the terms of an Attribution–Noncommercial–Share Alike–No Mirror Sites license for the first six months after the publication date (see <http://www.rupress.org/terms>). After six months it is available under a Creative Commons License [Attribution–Noncommercial–Share Alike 3.0 Unported license, as described at <http://creativecommons.org/licenses/by-nc-sa/3.0/>].

dimers to the point of coat formation on the ER membrane to form the so-called inner coat. A heterotetramer of Sec13/Sec31 is subsequently organized around this inner coat to form an outer coat. These polymerize into a latticelike structure that drives membrane curvature. The stochastic sampling model predicts that the cargo enters the vesicles by bulk flow, thus allowing for sampling of the contents of the lumen and membrane by chance. This could explain the transport of abundant cargo molecules but is insufficient to explain cargoes that get enriched in the vesicles beyond their existing concentration (Pfeffer and Rothman, 1987; Pelham, 1989; Balch et al., 1994; Klumperman, 2000; Barlowe and Miller, 2013). The selective cargo capture scheme involves direct interaction of the cargo with the coat proteins via the cargo ER exit signals or, in the case of some soluble secretory proteins, could entail the utilization of cargo receptors that would recognize the cargo and link them to the coat proteins. Proteins such as Erv29p in yeast and Tango 1 in mammals couple secretory cargo molecules to the COPII coat (Belden and Barlowe, 2001; Saito et al., 2009).

Enzymatic activity of phospholipase D and enrichment of phosphatidic acid at the ER exit sites have implied a role for lipids in COPII vesicle budding (Pathre et al., 2003). Phosphatidic acid phospholipase A1 (PAPLA1) enzymes hydrolyze the ester bond at the *Sn-1* position. The mammalian intracellular PAPLA1 family is comprised of three members. DDHD1, the canonical cytosolic PAPLA1, was purified from bovine testis based on its ability to deacylate phosphatidic acid at *Sn-1* position to generate fatty acid and *Sn-2* lysophosphatidic acid (Higgs and Glomset, 1996). DDHD2 or KIAA0725p is present in the Golgi/ER–Golgi intermediate, and its knockdown in tissue culture cells can retard the transport of VSVG from the Golgi apparatus (Sato et al., 2010). Sec23-interacting protein (Sec23IP; or p125) is a homologue of PAPLA1, and its interaction with Sec23 and Sec31 suggested a potential role for this protein in the assembly of COPII proteins and thus a possible role in protein transport (Shimoi et al., 2005; Ong et al., 2010). However, a function for this protein or its homologues in transport of specific cargo has not been demonstrated. Mutations in DDHD1 and DDHD2 are associated with hereditary spastic paraparesis in humans (Schuurs-Hoeijmakers et al., 2012; Tesson et al., 2012; Fink, 2013; Gonzalez et al., 2013). The target proteins, if any, compromised in these mutants have yet to be identified. A mouse null mutant for the p125 protein was recently reported, and the mutant male mice are subfertile (Arimitsu et al., 2011). Again, a specific function for this protein in protein transport was not described in the study.

In this study, we delineate a transport function for the PAPLA1 homologue in *Drosophila melanogaster*. Our study shows that PAPLA1 is an authentic PAPLA1 and a protein that interacts with members of the COPII carriers. We have generated a null mutant for this gene and show that the mutant affects several N-linked glycosylated G protein–coupled receptors (GPCRs), including Rh1 (rhodopsin 1) and Boss (Bride of sevenless). Genetic epistasis experiments and cell biological analysis show that the steady-state levels of Rh1 are compromised with an altered glycosylation pattern. We show that these changes are caused by defects in transport between the ER and the

Golgi complex. Steady-state and pulse–chase experiments, *in vivo*, show that a significant fraction of the newly synthesized Rh1 is ectopically localized and unstable in the mutant. The defective transport of Rh1 contributes to the progressive decline in steady-state levels of Rh1 in the flies, leading to decreased ability of the mutants to transduce light signal. In addition, the mutant flies show other phenotypes, such as male sterility, increased starvation sensitivity, and locomotor defects. Our experiments support the conclusions that the PAPLA1 protein is required for the physiological transit of a family of N-linked glycosylated proteins from the ER to the Golgi complex.

## Results

### CG8552 is a PAPLA1

Sequence analysis indicated that PAPLA1 gene CG8552 is the only homologue in *Drosophila*. Multiple sequence alignments and phylogenetic analysis showed that DDHD1 and CG8552 share a common ancestor, and DDHD2 and Sec23IP (p125) evolved from an even earlier ancestor (Fig. 1 A). A 31-kb genomic fragment modified to carry a V5 epitope at the N terminus of the PAPLA1 (V5-N-PAPLA1) protein was fully functional in *Drosophila* and rescued all the phenotype of a null mutant (see later in this paper and Fig. S3, A and B). These flies were used in immunofluorescence experiments for subcellular localization of the endogenous PAPLA1 protein. To determine the subcellular distribution of the protein accurately, we were able to use a demonstration superresolution structured illumination microscope (SR-SIM; ELYRA S1 [Carl Zeiss]). The protein showed strong colocalization with the Sec23 protein in a number of tissues, including oocyte and male accessory gland (Fig. 1, B and C). Sec23 and PAPLA1 colocalization was also detectable by confocal microscopy. Fig. S1 A is a confocal image of a section from the superficial layer of the accessory gland where the immunostained structures are slightly larger ( $71 \pm 12\%$  of clearly visible Sec23 signals overlapped with PAPLA1, and  $75 \pm 13\%$  of PAPLA1 signals overlapped with Sec23). We were able to demonstrate the presence of Sec23 in immunoprecipitates of the V5-tagged PAPLA1 from *Drosophila* head extracts (Fig. 1 D). Sec23 protein is enriched at the ER exit sites, a cytoplasmic zone between the transitional ER and the Golgi complex, where it is associated with a population of vesicles and tubules (Kondylis et al., 2007). PAPLA1's localization is also distinct from Lava lamp, a peripheral Golgi protein (Fig. S1 B; Sisson et al., 2000). A stable S2 cell line expressing a C-terminally V5-tagged PAPLA1 was established, and Flag-tagged *Drosophila* Sec23 and Sec31 were individually expressed in this cell line. Immunoprecipitation experiments of the V5-tagged PAPLA1 showed direct interaction between PAPLA1 and Sec23 and also between PAPLA1 and Sec31 (Fig. S1 C). These results are reminiscent of the interaction of mammalian p125 proteins with the COPII complex (Tani et al., 1999; Ong et al., 2010). Thus, the subcellular localization of PAPLA1 and its interactions raise the possibility that PAPLA1 could play a role in trafficking of proteins between ER and the Golgi complex. To ascertain whether the protein displayed enzymatic activity, we generated transgenic flies expressing PAPLA1 using the upstream activating

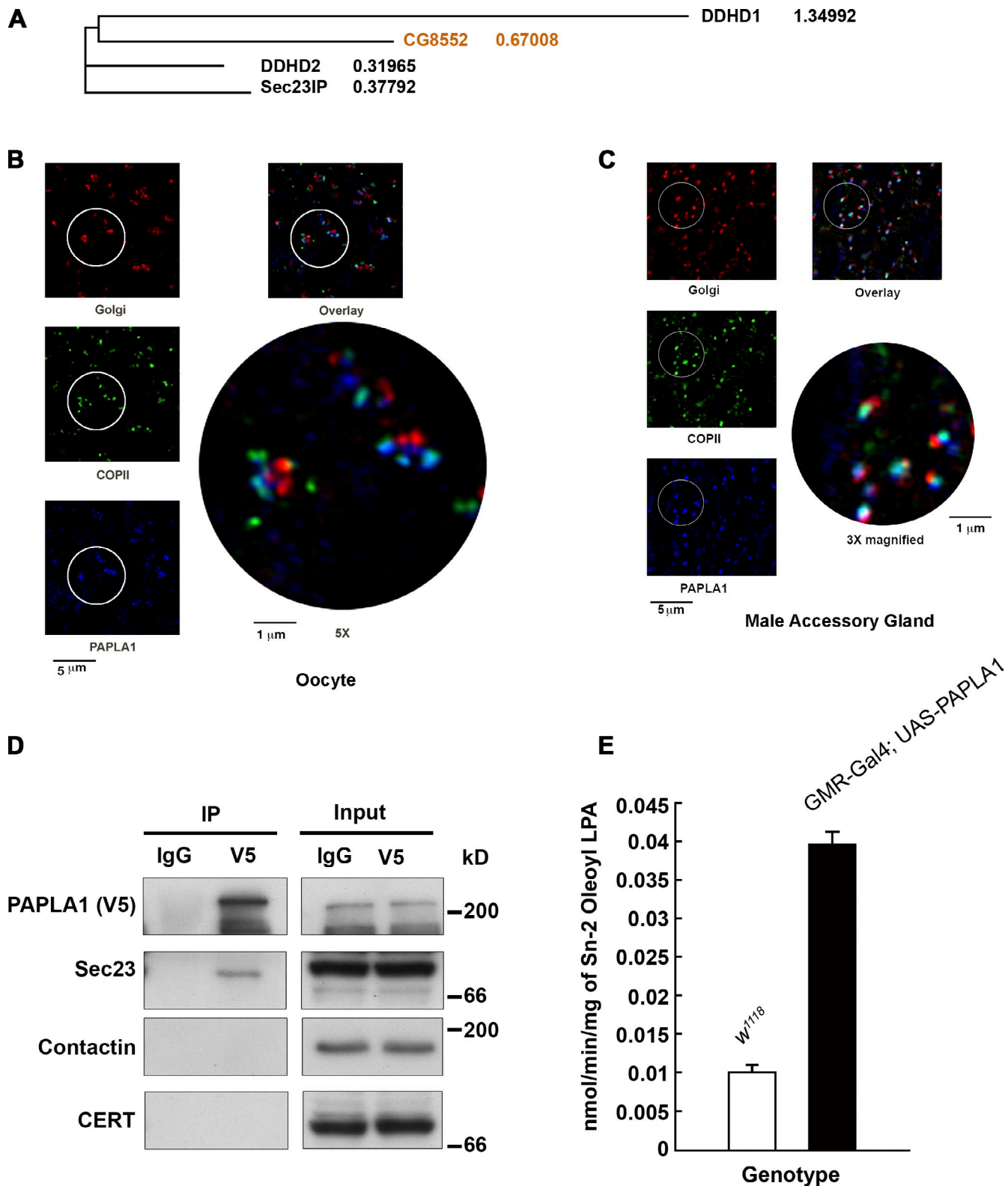


**Figure 1. Homology, localization, interaction, and enzymatic activity of PAPLA1.** (A) Cladogram of the DDHD1, DDHD2, Sec23IP (human), and CG8552. The numbers indicate the tree distance. (B and C) SR-SIM of the *Drosophila* female oocyte (B) and male accessory gland (C). The Golgi was probed with a monoclonal antibody raised against a 120-kD Golgi-integral membrane protein. (D) The Sec23 protein is detectable in immunoprecipitates of PAPLA1 from *Drosophila* heads. Contactin and CERT serve as negative controls. (E) PAPLA1 activity measured in extracts from control and PAPLA1-overexpressing *Drosophila* head extracts. The error bars indicate standard error of the means. IP, immunoprecipitation; LPA, lysophosphatidic acid.

sequence (UAS)-GAL4 system in the eye. Fly extracts containing the overexpressed protein showed a significant increase in the PAPLA1 activity compared with the control (Fig. 1 E). Incidentally, the mammalian p125 that colocalizes with Sec23 lacks the enzymatic activity (Nakajima et al., 2002). On the other hand, both DDHD1 and DDHD2 demonstrate phospholipase A1 activity (Higgs and Glomset, 1996; Nakajima et al., 2002). Thus, the lone *Drosophila* PAPLA1 protein could encode functions that overlap with all three mammalian family members.

#### GPCRs are compromised in a PAPLA1-null mutant

The CG8552 gene is localized to the left arm of the second chromosome and is encoded by a 25-kb (25,328 bp) gene with seven exons. It translates into a protein containing 2,016 amino acids with an N-terminal proline-rich region, a WWE domain, and a C-terminal DDHD domain (Fig. 2 A). The protein is considerably longer than the three mammalian homologues. Much of the homology with the mammalian proteins is confined to the C-terminal 700 amino acids. The N-terminal proline-rich region shows no significant homology with known mammalian proteins. To delineate a role for PAPLA1 in vivo, we generated a null deletion mutant using ends-out homologous recombination (Gong and Golic, 2003). The design of homology arms used for creation of the targeting vector and the nature of deletion is summarized in Fig. 2 B. The two exons retained in the mutant encode a protein of only 81 amino acids, and thus, the mutant flies are functionally null for all practical purposes. *Drosophila* phototransduction has served as a good model for the study of protein trafficking as well as posttranslational modification of proteins and membrane turnover experiments. Therefore, we analyzed *Drosophila* head extracts to probe for proteins of phototransduction in the hope of unraveling clues to the transport function for PAPLA1, if any. Previous studies in mutant mouse and tissue culture cells had failed to identify specific targets that were affected by DDHD1, DDHD2, or the p125 protein (Arimitsu et al., 2011; Schuurs-Hoeijmakers et al., 2012; Tesson et al., 2012; Gonzalez et al., 2013). We found a consistent and significant decrease in the levels of rhodopsin (Rh1) in Western blots from *papla1* mutant head extracts compared with wild-type controls, and the residual Rh1 also exhibited a slightly higher apparent molecular mass (Fig. 2 C). Other phototransduction components, such as NorpA (No receptor potential A), transient receptor potential (Trp), and NinaC, were not significantly affected in the mutants (Fig. S1 D). The decrease in Rh1 levels and the altered molecular mass were observed when the flies were either exposed to light (in a day/night pattern) or raised in total darkness (Fig. S2, A and B). These results indicate that changes in the apparent molecular mass and steady-state levels of Rh1 in *papla1* mutants were not likely a result of the activation and involvement of the phototransduction cascade (such as increased Rh1 turnover after endocytosis upon light-induced stimulation) but rather intrinsic to the properties of Rh1 rendered during either synthesis, posttranslational modification, or trafficking of the protein. The decrease in Rh1 was not caused by photoreceptor degeneration (Fig. 3 C). Depending on the age of the fly, the steady-state levels of Rh1 were decreased

between three- and fivefold in the mutant and were worse in the older flies (Fig. S2, A and B). Rh1 is a prototypic member of the GPCR family. It is expressed in R1–R6 photoreceptor cells and is the most abundant rhodopsin in flies. We inquired whether other rhodopsins were similarly affected in *papla1* mutants. Rh3 and Rh4 are minor rhodopsins expressed in nonoverlapping sets of R7 photoreceptor cells. Rh5 and Rh6 are expressed in nonoverlapping sets of R8 cells. The endogenous levels of these proteins are very low, and available monoclonal antibodies did not detect these proteins in Western blots. Therefore, we used transgenic flies that express Rh3 and Rh5 proteins in R1–R6 cells under the Rh1 promoter. The use of the Rh1 promoter expands the expression of Rh3 and Rh5 to R1–R6 cells and renders them visible by immunoblot analysis. We probed for ectopically expressed Rh3 and Rh5 by Western blot analysis in both the wild-type control and the *papla1* mutant fly background. Like with Rh1, the levels of Rh3 and Rh5 were greatly reduced in the mutant compared with the control flies (Fig. 2, D and E). Thus, the loss of PAPLA1 affects the steady-state levels of several rhodopsins in *Drosophila*. Finally, we explored whether a GPCR other than rhodopsin was affected in the *papla1* mutant. Boss is a GPCR originally identified as a ligand for the receptor tyrosine kinase sevenless in determining the fate of R7 cells in developing ommatidia of *Drosophila* (Hart et al., 1990). A recent study showed that in adult flies, Boss also responds to extracellular glucose and regulates sugar and lipid metabolism (Kohyama-Koganeya et al., 2008). Our analysis indicates that levels of the Boss protein were also decreased in the *papla1* mutant (Fig. 2 F). The decline worsens with aging, and older flies have almost a fourfold decrease in the steady-state levels of the protein compared with the controls (Fig. S2 C). We checked whether PAPLA1 would be required for the transport of other N-glycosylated proteins. Contactin is a glycosylphosphatidylinositol-anchored cell adhesion molecule that contains immunoglobulin domains linked to fibronectin type III repeats and is N-glycosylated (Faivre-Sarrailh et al., 2004). This protein is predominantly expressed in the neurons and is implicated in control of axonal growth. Western blot analysis showed that neither the protein levels nor the apparent molecular mass of contactin was affected in the *papla1* mutant. Thus, contactin is not compromised in the *papla1* mutant (Fig. S2 F). Neurogian is an integral membrane protein and a cell adhesion molecule expressed in the central nervous system and is also N-glycosylated (Bieber et al., 1989). We were unable to observe discernable changes in the levels or molecular mass of neurogian from the *papla1* mutant (Fig. S2 G). Thus, the deficiency of PAPLA1 protein selectively affects the steady-state levels of a subset of GPCR family members in *Drosophila*.

As mentioned previously in this paper, Rh1 is not only decreased in the mutant flies but is also of slightly higher molecular mass (by ~2–3 kD; Fig. 2 C). Indeed, changes in the apparent molecular mass were observed in other proteins too. Unlike Rh1, the apparent molecular mass of the Boss protein in the mutant was slightly lower than in the wild-type control (Fig. 2 F and Fig. S2, C–E). The difference in the steady-state levels and apparent molecular mass of the proteins in the wild-type control and the mutant flies indicates

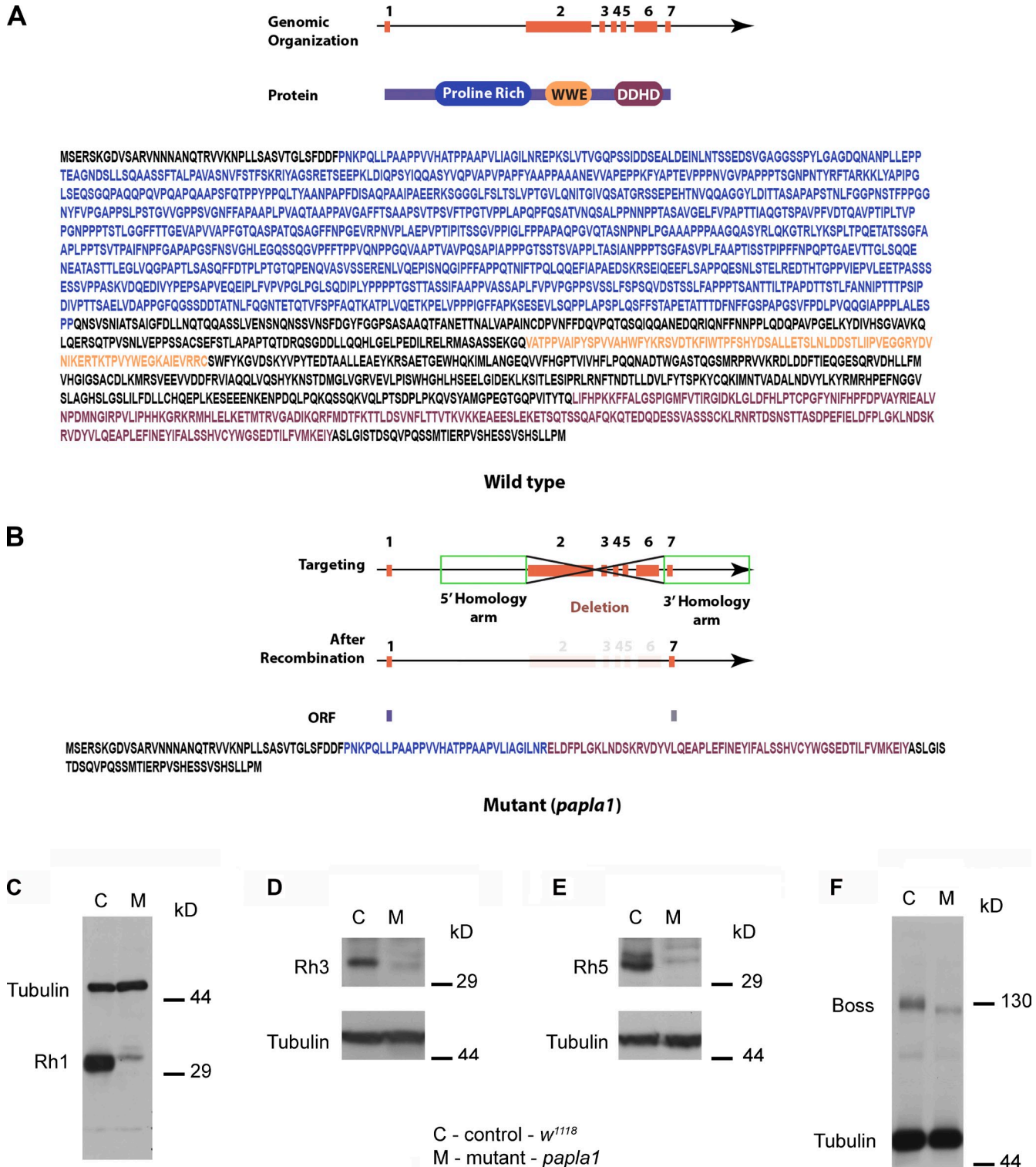


**Figure 2. *papla1*-null mutant affects the integrity of several of GPCRs.** (A) The genomic organization (top), the protein domains (bottom), and the protein sequence of PAPLA1. (B) The green box in the top drawing represents the homology arms used for generation of the *papla1*-null allele, and the middle shows the exons retained in the null mutant. The bottom shows the encoded protein in the *papla1* mutants. (C-F) Western blots of head extracts from the control and *papla1* mutant flies probed with anti-Rh1 (C), Rh3 (D), Rh5 (E), and Boss (F).

that the deficiency of PAPLA1 compromises the fate of several GPCRs.

In microsomal preparations, a small fraction of the Rh1 was found to immunoprecipitate with PAPLA1 in vivo (see

Fig. 5 E). Also, in S2 cells, transiently expressed PAPLA1 co-immunoprecipitated with the Boss protein, indicating a physical interaction between PAPLA1 and the two GPCRs (Fig. 5 F). Although these experiments indicate a physical interaction, we do

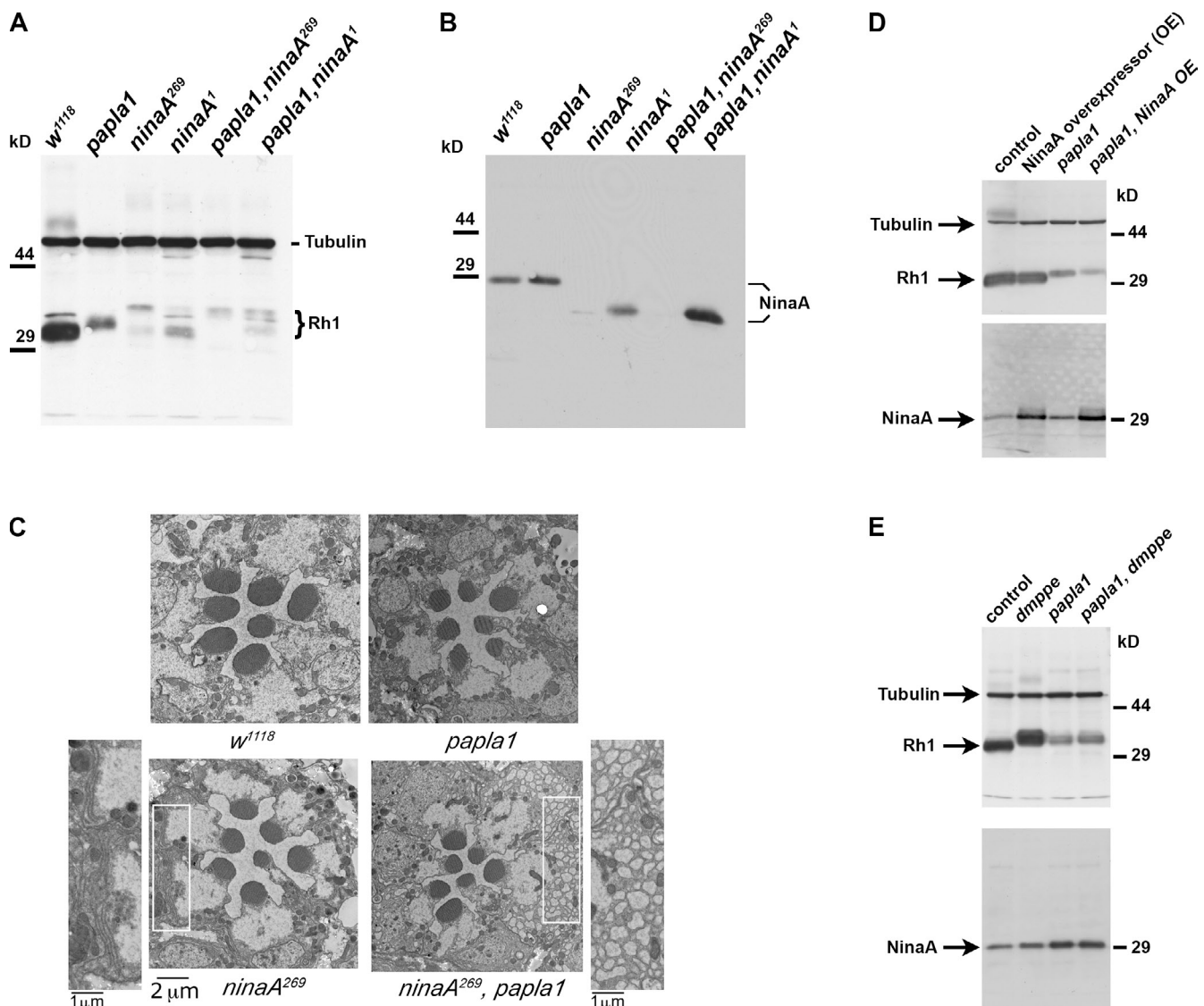


**Figure 3. PAPLA1 acts downstream of the Rh1 chaperone NinaA and upstream of the Golgi-resident protein dMPPE.** (A) Western analysis of single head extracts from control, *papla1*, *ninaA<sup>269</sup>*, *ninaA'*, *papla1-ninaA<sup>269</sup>* double mutant, and *papla1-ninaA'* double mutant flies. (B) The same blot was probed with the NinaA antibody. NinaA protein levels are increased in all of the *papla1* mutant backgrounds that have a functional NinaA protein, including the *ninaA'*-*papla1* double mutants. (C) Electron microscopy from the control, *papla1*, *ninaA<sup>269</sup>*, and *ninaA<sup>269</sup>-papla1* double mutant backgrounds. The boxed regions shown in *ninaA<sup>269</sup>* and *ninaA<sup>269</sup>-papla1* double mutants have been enlarged. (D) Increased expression of NinaA in *papla1* mutants does not result in increased steady-state levels of Rh1. Single fly head extracts of newly eclosed flies of the appropriate genotype were probed for Rh1, tubulin, and NinaA. The same blot was probed for all three antibodies. (E) Western blots of protein extracts from control and *dmppe* mutant flies. The same blot was probed for all three antibodies.

not know whether this is a direct physical interaction or if they are part of a larger complex. Because Rh1 is a well-studied protein and phototransduction cascade has been intensively investigated, we decided to focus on this protein to probe deeper into the defects observed in the N-linked GPCR family in *papla1* mutants.

#### PAPLA1 is required for the ER to Golgi transit of Rh1

The Rh1 protein is synthesized in rough ER and is glycosylated initially to a 40-kD high molecular mass form that then undergoes progressive deglycosylation along the secretory pathway, including the Golgi complex. NinaA (Neither inactivation nor after potential) protein is a peptidyl-prolyl cis-trans isomerase that initiates function as a chaperone in the ER during the folding

and transport of Rh1. We found that the steady-state levels of NinaA were always higher in the mutant compared with wild-type controls, perhaps indicative of incipient ER stress in *papla1* mutants (Fig. 3, Fig. S1 D, and Fig. S3 C). We decided to examine the epistatic relation between *ninaA* and *papla1* in the hope it would enable us to genetically dissect the point of action of PAPLA1 protein during the synthesis and transport of Rh1. We used two *ninaA* mutant alleles for genetic epistasis experiments.

In *ninaA<sup>269</sup>* (*ninaA<sup>3</sup>*) mutants, Rh1 levels are low, and most of the residual Rh1 appears as a nearly 40-kD protein that accumulates in the ER (Fig. 3 A; Colley et al., 1991; Webel et al., 2000). This mutant has an H227L mutation in the NinaA protein, which renders it extremely unstable, the flies show very

little mature Rh1 in the rhabdomere, and much of the Rh1 is in the immature form in the ER (Colley et al., 1991; Webel et al., 2000). The mutant flies also show proliferation of the ER (Fig. 3 C; Colley et al., 1991). The second mutant *ninaA*<sup>1</sup> encodes a truncated NinaA (W208\*) that is partially active at room temperature and is a temperature-sensitive allele (Colley et al., 1991). In these flies, Rh1 is of normal molecular mass, but its levels are reduced at 25°C (Fig. 3 A).

In *ninaA*<sup>269</sup>-*papla1* double mutants, the Rh1 levels are low, and the residual Rh1 is ~40 kD, similar to the phenotype of *ninaA*<sup>269</sup> allele, thus demonstrating that NinaA acts upstream of PAPLA1 (Fig. 3, A and B). If this is true, we predict that in a double mutant of *papla1* and the hypomorphic *ninaA*<sup>1</sup>, the small amount of mature Rh1 observed in the *ninaA*<sup>1</sup> hypomorph will now migrate as in a *papla1*-null fly. Indeed, in the *ninaA*<sup>1</sup>-*papla1* double mutant in which NinaA is still partially active, the apparent molecular mass of the mature Rh1 shifts to that observed in *papla1*. As in *papla1* mutants, we also observe up-regulation of the truncated NinaA protein in the *ninaA*<sup>1</sup>-*papla1* double mutant (Fig. 3 B). It is worth noting that, in the *ninaA*<sup>269</sup>-*papla1* double mutant, we saw severe dilation of the ER, indicating that the ER stress observed in *ninaA*<sup>269</sup> mutants (manifested as proliferation of ER) is exacerbated when PAPLA1 is lost in these flies (Fig. 3 C). The genetic epistasis data, the colocalization of PAPLA1 with Sec23 protein, and the ER dilation observed in the *ninaA*<sup>269</sup>-*papla1* double mutants together suggest that PAPLA1 acts immediately downstream of the site of action of NinaA in the immediate proximity of the ER, during the transport of Rh1. Because NinaA protein levels were increased in the *papla1* mutant and NinaA is a known chaperone for Rh1 protein, we wondered whether the increased levels of NinaA were used for stabilizing the immature Rh1 found in the *papla1* mutant or whether it was an indicator of an underlying ER stress. If the increased NinaA is stabilizing the residual Rh1 in the *papla1* mutant, overexpression of the protein should stabilize and increase the Rh1 levels. To test this, we generated NinaA transgenic flies and specifically overexpressed them in the photoreceptor cells using the long glass multimer reporter-Gal4 driver lines (Wernet et al., 2003). Increased expression of NinaA, however, did not increase the levels of Rh1 in the *papla1* mutant. These results support the notion that incipient ER stress in *papla1* may be responsible for the up-regulation of NinaA protein levels, but increasing the NinaA levels does not result in increased steady-state levels of Rh1 in *papla1* mutants (Fig. 3 D).

Because PAPLA1 colocalizes with components of COPII coat proteins, which are enriched at the ER exit sites, we predict that the *papla1* phenotype will dominate over that of a mutant for a Golgi-resident protein involved in Rh1 transport. dMPPE (CG8889) is a Golgi-resident metallophosphoesterase that dephosphorylates  $\alpha$ -Man-II ( $\alpha$ -Mannosidase II) and activates it (Cao et al., 2011). In *CG8889*<sup>02905</sup> (*dmppe*), a mutant of CG8889,  $\alpha$ -Man-II, remains phosphorylated and is inactive. Because  $\alpha$ -Man-II is inactive in the Golgi, the Rh1 that transits through the Golgi in this mutant is not deglycosylated by  $\alpha$ -Man-II. The additional sugar residues on Rh1 in the *dmppe* mutant increase the molecular mass of the protein slightly, but the steady-state level of Rh1 is not significantly altered in the

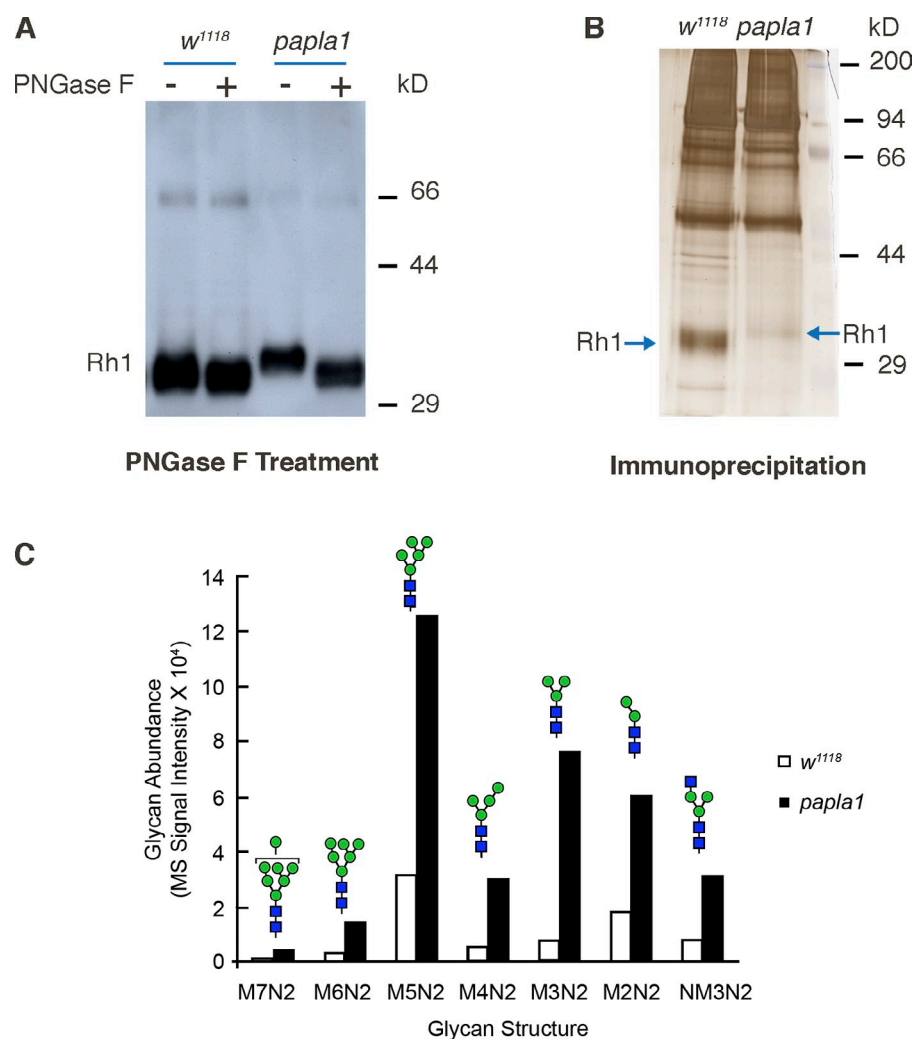
mutant. Because the Rh1 in the *papla1* mutant is also of a similar molecular mass as in the *dmppe* mutant, we performed genetic epistasis experiments to evaluate whether PAPLA1 acts upstream of dMPPE, the Golgi-resident enzyme. We generated a *papla1-dmppe* double mutant and tested the Rh1 levels by Western blot analysis. As seen in Fig. 3 E, the apparent molecular mass of Rh1 is similar in both the *dmppe* and *papla1* mutant, and they are both slightly larger than wild-type Rh1. Although the amounts of Rh1 in wild-type control and *dmppe* are comparable, the *papla1-dmppe* double mutant retains the phenotype of *papla1* because the Rh1 levels are reduced to that observed in *papla1* mutant, indicating that most likely PAPLA1 acts upstream of dMPPE. Furthermore, the degree of reduced SDS-PAGE mobility observed in the *dmppe* single and *dmppe-papla1* double mutant is similar to the shift observed in the *papla1* single mutant, suggesting that both mutations may impact the same glycan processing step.

The aforementioned genetic experiments indicate that PAPLA1 acts downstream of NinaA. Our observations also suggest that it acts upstream of dMPPE, in the maturation of Rh1 in *Drosophila* photoreceptors. Combined with the findings from immunolocalization and coimmunoprecipitation experiments described previously in this paper, we believe that PAPLA1 acts along the ER–Golgi axis either at the ER exit sites or at the ER–Golgi contact point and is required for the anterograde trafficking of Rh1 from the ER to the Golgi complex.

#### PAPLA1 is required for Golgi processing of the GPCRs

In the wild-type control flies, the ER glycosylated Rh1 is either extensively trimmed or completely divested of sugar residues in the Golgi complex before being delivered as a mature protein (with an apparent molecular mass of 32 kD) to the rhabdomere (Huber et al., 1990; Katanosaka et al., 1998). The molecular mass of Rh1 in the *papla1* mutant is similar to those reported for *dmppe* and  $\alpha$ -Man-II mutants, in which the deglycosylation of Rh1 in the Golgi complex is compromised (Walther and Pichaud, 2006). Rh1 undergoes core N-linked glycosylation in the ER, and these glycosyl moieties undergo processing as the protein transits from the ER through the Golgi complex to the rhabdomere (Katanosaka et al., 1998; Webel et al., 2000). To evaluate whether the observed difference in Rh1 was a result of a lack of processing of glycosyl residues in the Golgi complex, we subjected Rh1 from both control and mutant extracts to peptide N-glycosidase F (PNGase F) treatment. PNGase F cleaves between the innermost GlcNAc and asparagine residues of N-linked glycoproteins (Maley et al., 1989). If the difference in apparent molecular mass of the Rh1 in mutants was caused by defects in glycosylation, treatment with PNGase F should yield Rh1 proteins of similar molecular masses in both the control and the mutants. Indeed, PNGase F treatment of wild-type and mutant extracts results in Rh1s that are indistinguishable by molecular mass (Fig. 4 A). These results indicate that the observed difference in the molecular mass was caused by altered glycosylation patterns of Rh1 in the two genetic backgrounds. We also wanted to test whether the other GPCR, Boss, showed a similar glycosylation defect. Boss is also an N-linked

**Figure 4. The increased apparent molecular mass of Rh1 in the *papla1* mutant is caused by defective deglycosylation.** (A) Western blot analysis of Rh1 molecular masses before and after treatment with PNGase F in control *w<sup>1118</sup>* and *papla1* mutants. (B) Immunoprecipitates of Rh1 from control *w<sup>1118</sup>* and *papla1* mutants. The decreased amounts and higher molecular masses of the immunoprecipitated proteins can be appreciated in the silver-stained gels. Quantification by densitometry indicates that the *papla1* mutant has greater than eightfold less Rh1 than wild type. (C) Mass spectrometric analysis of N-glycans linked to Rh1 in wild-type and *papla1* mutant heads. N-linked glycans were released from Rh1, which was immunoprecipitated from 100 wild-type or 500 *papla1* head extracts. (blue squares, N-acetylglucosamine; green circles, mannose), and the labels along the x axis refer to the composition of the glycan based on number of mannose residues (M) and number of N-acetylglucosamine residues (N). The MS samples were run in triplicates with identical results. The biological experiment was completed once with pooled Rh1 as described in the Results section describing the glycosylation patterns observed in mutant and wild-type Rh1.



glycoprotein, and a monoclonal antibody was able to detect a small but consistent difference in the molecular mass of the protein in the wild-type and mutant background (Fig. S2, C–E). However, in this instance, the observed molecular mass of the mutant protein is lower than the wild type. Because Golgi processing can either remove or add additional sugars, it is likely that in the case of Boss, the modifications that occur in the Golgi in the wild-type flies result in increased oligosaccharide chain lengths. Like with Rh1 proteins, PNGase F treatment results in Boss proteins of similar molecular masses from the two backgrounds (Fig. S2 H).

To evaluate the extent of glycosylation of Rh1 expressed in wild type and the *papla1* mutant, we performed N-linked glycan analysis by mass spectrometry (MS). Rh1 was immunoprecipitated from 100 wild-type and 100 mutant heads using the 4C5 antibody (Fig. 4 B). After silver stain of the immunoprecipitated material, the Rh1 levels were quantified by densitometric scanning and found to be more than eightfold less in the mutant compared with wild type. Therefore, to obtain sufficient material from the *papla1* mutant, Rh1 was immunoprecipitated from 500 total mutant heads for comparison with Rh1 precipitated from 100 wild-type heads. Thus, despite precipitating from fivefold more mutant heads, the total Rh1 harvested from the *papla1*

mutant would be conservatively expected to be less, based on silver staining. After SDS-PAGE and silver staining of the immunoprecipitations, Rh1 bands were excised away from the rest of the gel, and the resulting gel pieces were subject to in-gel tryptic digestion. N-linked glycans were released from the glycopeptides by PNGase F digestion and further analyzed by MS as their permethylated derivatives. Despite the lower amount of Rh1 obtained from *papla1* mutant heads, the abundance of total N-linked glycans was substantially greater (Fig. 4 C). Among the major glycans detected by our analysis, the  $\text{Man}_5\text{GlcNAc}_2$  structure (M5N2) dominated the profile in both wild types and the *papla1* mutant. The M5N2 glycan is the substrate for the Golgi  $\alpha$ -Man-II enzyme that is inactivated in the *dmppe* mutant (Fig. 3 E). Therefore, the increase in M5N2 in the *papla1* mutant is consistent with decreased Golgi processing of Rh1. The oligosaccharide chain in mature Rh1 from control photoreceptors would be extensively trimmed or completely removed, and hence, there are fewer glycosylated chains in the eluate (Huber et al., 1990; Katanosaka et al., 1998). Thus, any glycosylated Rh1 evaluated in the control would be the small amounts of immature Rh1. Indeed, all of the major N-linked glycans detected on wild-type Rh1 were substantially increased in abundance on Rh1 from *papla1*, which is consistent with hyperglycosylation

of this protein in the mutant. Thus, the observed defects in molecular mass are a result of lack of processing of the N-linked glycosylated GPCRs Rh1 and Boss by Golgi enzymes in the *papla1* mutant.

### Rh1 demonstrates aberrant localization in the *papla1* mutant

Confocal microscopic localization of Rh1 showed that in the wild-type R1–R6 photoreceptor cells, much of the Rh1 localizes to the base of the rhabdomere, along with punctate staining thought to be of multivesicular bodies of endocytosed Rh1 and some perinuclear staining perhaps indicative of newly synthesized Rh1 in the ER (Fig. S3 A, left images). However, a considerable amount of Rh1 was mislocalized in the *papla1* mutant (Fig. S3 A, middle images). Although some Rh1 was retained at the base of the rhabdomere, a significant fraction of the protein was targeted to other areas of the cell. This defect is restored in the rescued flies (Fig. S3 A, right images).

To determine whether transport of Rh1 was compromised in the *papla1* mutant, we followed the synthesis and transport of newly synthesized Rh1 in vivo using the heat shock (hs)–Rh1-1D4 transgene using a pulse–chase paradigm. In flies carrying a copy of the transgene, Rh1 can be induced in photoreceptor cells under the control of an hs promoter that is activated at 37°C. The Rh1 is tagged with a sequence from the bovine opsin, termed Rho-1D4 at its C terminus (hs-Rh1-1D4; Colley et al., 1995). Thus, the synthesis and fate of the hs-induced tagged Rh1 can be followed independent of endogenous Rh1 using a monoclonal antibody against Rho-1D4. The expressed Rh1-1D4 is fully functional and rescues the Rh1-null mutant (*ninaE*<sup>117</sup>) phenotype (Colley et al., 1995). We recombined this transgene into the wild-type and *papla1* mutant background and followed the fate of newly synthesized Rh1 by Western blot analysis and immunofluorescence imaging. Western blot analysis showed that in the control flies, a pulse of 1-h hs results in the generation of a mature protein that is clearly visible in Western blots by ~12 h, and the Rh1 is stable at least for 24 h (Fig. 5 A). On the other hand, in *papla1* mutants that were similarly treated, Rh1 was always of higher molecular mass than in controls and was consistently in lower amounts. To follow the subcellular localization of the newly synthesized Rh1, we performed whole-mount retinal staining of *Drosophila* ommatidia. Around 12 h after induction, we see clear staining of the rhabdomeres in the wild-type control flies (Fig. 5 B). Although some Rh1 is visible in the rhabdomeres of the *papla1* mutant at this time point, it is faint and is only a fraction of the Rh1 synthesized in the mutant. A significant fraction of the protein is ectopically localized in these mutants (Fig. 5 B). In fact, 8 h after induction, Rh1 began to accumulate in the rhabdomere of the wild-type controls (Fig. S4 A). In the mutant, on the other hand, we observed that the newly synthesized Rh1 was being targeted to other areas of the cell, and only a small amount was being delivered to the rhabdomere (Fig. S4 B). The rhabdomere staining was still visible in all the wild-type controls examined ~24 h after the hs, whereas in the mutant, many of the eyes examined exhibited little signal in the rhabdomere at this time (Fig. S4, C and D). Because by 8 h most of the Rh1 is localized to the rhabdomere

in wild-type controls, we performed colocalization experiments with *papla1* mutants at 10 h to observe the subcellular location of Rh1. In the mutant, the ectopic Rh1 predominantly colocalized with calnexin, an ER-resident protein. No significant colocalization was observed with Rab7 (Fig. S5, A and B). The pattern of Rh1 staining was similar to that observed in *ninaA*<sup>269</sup> (Fig. S5 C). Rh1 has been shown to colocalize with Golgi markers during the early stages of rhodopsin biosynthesis in developing pupae (Cao et al., 2011). We used these flies to colocalize the Rh1 and the Golgi complex in the wild-type and mutant backgrounds. For these experiments, we fixed flies 4 h after 1 h of hs induction and performed immunolocalization experiments for Rh1 and a Golgi marker. Although we saw partial colocalization of Rh1 with the Golgi marker in wild-type flies, we did not see colocalization of the Rh1 and the Golgi marker in the mutant (Fig. 5 C).

We recombined V5-N-PAPLA1 rescued flies to hs-Rh1-1D4 lines and examined whether we could colocalize PAPLA1 and Rh1. For this experiment, we induced the production of Rh1 with hs at 37°C for 2 h and performed the whole-mount immunostaining of the eye with antibodies against Rho-1D4 and V5, 2 h after the hs. Under these conditions, dispersed between the reticular staining of Rh1, we see a faint but distinct overlap of signals from PAPLA1 and Rh1, and together with the results from immunoprecipitation experiments described previously in this paper, these data suggest that the two proteins could interact (Fig. 5 D–F).

### The active site of PAPLA1 is not necessary for Rh1 maturation

Transgenic overexpression of PAPLA1 results in increased enzymatic activity. Also, a 31-kb genomic construct containing either untagged or N-terminal V5 epitope-tagged PAPLA1 was able to rescue all the phenotypic defects observed in *papla1* mutants (Fig. S3, A and C). To evaluate whether phospholipase A1 activity was necessary for its function in the eye, we generated a transgenic construct based on the untagged genomic rescue construct but with mutations in the five residues critical for the enzymatic activity. Lipases and esterases share a short consensus sequence, GXSXG. The pentapeptide is located at the active site of these enzymes, and the serine is part of the Ser-Asp-His catalytic triad of the enzyme (Derewenda, 1994). PAPLA1 contains the sequence GHSLG at residues 1,682–1,686 of the protein. Site-directed mutagenesis in several lipases showed that the serine residue within the GXSXG sequence was the acylated center of the lipase gene family and was essential for catalytic activity (Davis et al., 1990; Emmerich et al., 1992; Lowe, 1992). Thus, to generate an enzyme lacking the lipase activity, we generated a PAPLA1 genomic construct without the pentapeptide consensus sequence. We deleted residues 1,682–1,686 (Δ1,682–1,686-PAPLA1) in the fifth exon of the gene in this transgenic construct using GalK-mediated recombineering. This protein was expressed in S2 cells, and the immunoisolated protein showed only baseline activity, indicating that the active site mutant was catalytically inert (Fig. S3 D). Transgenic flies carrying this active site mutant genomic rescue construct were recombined into the *papla1* mutant background. We then

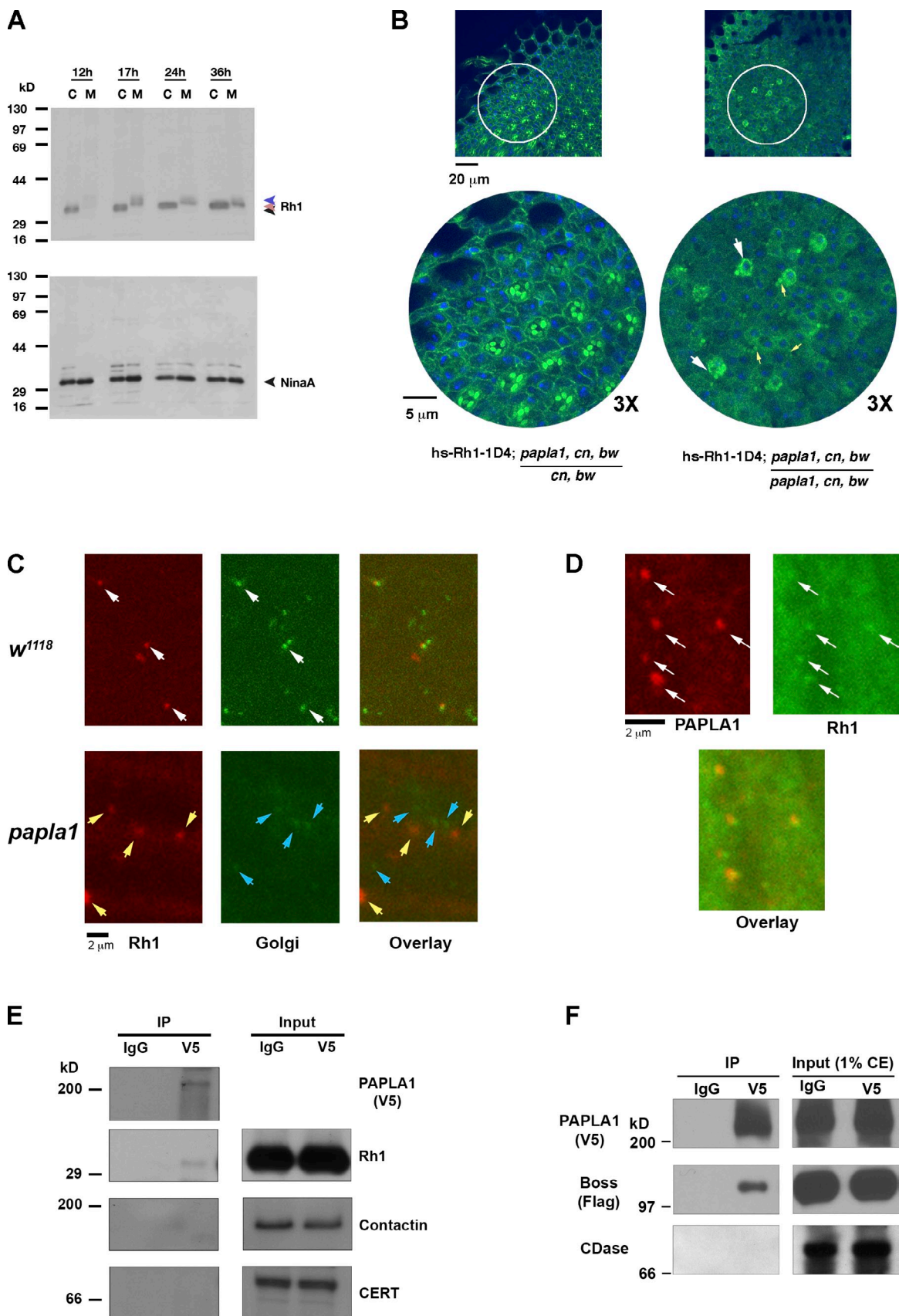


**Figure 5. Rh1 is mislocalized in *papla1* mutants.** (A) In hs-Rh1-1D4 transgenic flies, Rh1 synthesis can be initiated by a pulse of hs at 37°C, and only the induced Rh1 can be detected by using a 1D4-specific monoclonal antibody. The pink and purple arrowheads highlight the immature forms of Rh1. C, control; M, mutant. (B) Immunofluorescence imaging performed on 12-h control and mutant flies with hs-Rh1-1D4. The areas enclosed by the white circles

performed Western blot analysis of head extracts from these flies for Rh1 and compared them with *papla1* mutants and wild-type controls (Fig. S3 E). Unlike the mutant *papla1* alleles, the active site mutant fly-produced Rh1 protein is of similar molecular mass as the wild-type controls. Thus, the PAPLA1 protein lacking the critical active site residues was able to assist in the transport of Rh1 from the ER to the Golgi complex for proper maturation of the Rh1 protein in the flies. These experiments indicate that enzymatic activity was not crucial for the transport function of the PAPLA1 protein. Most likely, the protein–protein interaction of PAPLA1 with COPII components will likely play an important role in trafficking of selective proteins.

#### ***papla1* mutants display multiple phenotypes**

Because *papla1* mutants have a defective transport of several N-linked GPCRs, the consequences of lower steady-state levels of these proteins should compromise the viability of the mutant animals. Electroretinogram (ERG) recordings of 10-d-old *papla1* mutants show decreased sensitivity of the photoreceptor cells to light signal (Fig. 6 A). The amplitude of response of the mutant is less than half of the control flies at all light intensities tested by ERG. Although ERGs are never fully quantitative, this observation is in line with the low levels of Rh1 found in the mutant flies. *papla1* mutants are sensitive to starvation compared with the wild-type controls. The susceptibility of the mutants to starvation is very significant by day 10 and gets worse until about day 30 from when the difference remains the same (Fig. 6 B). Flies display an innate ability to climb up the walls of the vials they are housed in against the gravitational force (negative geotaxis). They harbor considerable segregating genetic variation for geotaxis behavior, and multiple additive quantitative trait loci contribute to this behavior. For these reasons, a negative geotaxis assay has generally been used to measure the vigor and vitality of flies. Because we propose that several GPCRs were compromised in the *papla1* mutant, we expected the flies to do poorly in this test. Indeed, 30-d-old flies fared poorly compared with age-matched controls, indicative of decreased vitality of the mutant flies (Fig. 6 C). The *papla1* mutant flies also have a 20% decreased life span (unpublished data).

The *papla1* mutants are male sterile. The testes of males are small compared with heterozygous and wild-type controls (Fig. 6 D). Fluorescence staining with DAPI demonstrated the existence of elongated spermatid bundles (Fig. 6 E, white arrows) along the testis in the control (Fig. 6 E, top) and the mutant (Fig. 6 E, bottom) flies. However, the individual needle-shaped nuclear staining of sperm found in the wild-type seminal vesicle (Fig. 6 E, top right) are absent in the mutants (Fig. 6 E, bottom right), indicating a defect in the individualization process

of spermatogenesis. Electron microscopic examination of testis showed that early stages of spermatogenesis, including the generation of the 64-cell spermatid bundle, seemed to occur in the mutant (Fig. 6 F). We see the clear formation of the major and minor mitochondrial derivatives and the formation of the axonemal structures in the bundles. However, closer examination of the spermatid bundles showed that the mitochondrial derivative and the process of individualization of the spermatids into sperms were defective in the mutants (Fig. 6 G). In many, the mitochondrial derivatives are not individualized and remain bridged between two spermatids. These defects lead to degeneration of the spermatids in the distal end of the testis. It is interesting to note that although the wild-type genomic construct rescues all of the phenotypes observed in the *papla1* mutant, the transgenic lines encoding the active site mutant do not rescue the male sterile phenotype observed in *papla1* mutants while restoring the maturation defect of Rh1, indicating that enzymatic activity is important for male fertility.

## **Discussion**

In this study, we have shown that PAPLA1, a cytosolic protein, is involved in the maturation of Rh1, an N-glycosylated GPCR, along the secretory pathway and is responsible for the transit of the ER-synthesized protein to the Golgi complex. GPCRs constitute the largest family of cell surface receptors and transduce a wide range of external stimuli in cells. The glycosylation of GPCRs has been demonstrated to be important for normal folding, trafficking, cell surface expression, stability, protein–protein interaction, and interaction with ligands in different GPCRs (Rademacher et al., 1988; Wheatley and Hawtin, 1999). In *papla1* mutants, the lack of processing of the protein by components of the Golgi complex is accompanied by two notable features (in addition to changes in glycosylation). First, the protein is mislocalized in the mutant cells (mostly in the ER), where normally we do not see the protein. Second, it probably affects the fate of the protein because we see a steady decline in the steady-state levels of the protein that tends to get worse in older flies. It is interesting to compare the fate of Rh1 in *papla1* (this study) and *dmppe* mutants (Cao et al., 2011). In *dmppe* mutants, Rh1 exhibits glycosylation similar to *papla1* mutants, at least at the level of SDS-PAGE mobility, yet Rh1 levels and rhabdomere targeting are not compromised. In both mutants, Rh1 is not deglycosylated by the Golgi  $\alpha$ -Man-II. In the case of *papla1*, Rh1 fails to reach the Golgi complex, whereas in the *dmppe* mutant, it traverses through the complex but does not undergo  $\alpha$ -Man-II-mediated deglycosylation. Thus, transit through the Golgi complex affords a great deal of stability

in the top images were enlarged threefold in the respective bottom images. (C) Rh1 colocalizes with a Golgi marker in the control  $w^{1118}$  cells, whereas we do not observe such colocalization in the *papla1* mutant photoreceptor cells. (D) Rh1 was induced in rescued *papla1* flies expressing V5-N-PAPLA1 and hs-Rh1-1D4 by a 2-h hs at 37°C and fixed after 2 h. (B–D) The white arrows show colocalization of Rh1 and Golgi markers in the wild type, whereas yellow arrows are Rh1 staining, and the blue arrows are Golgi staining in the *papla1* mutant photoreceptor cells. (E) The Rh1 protein is detectable in immunoprecipitates of PAPLA1 from *Drosophila* head microsomal preparations. Contactin and CERT were probed as negative controls. The amount of V5 in microsomal preparation was too low to be seen on 1% of crude extracts and is not depicted. (F) V5-tagged PAPLA1 and Flag-tagged Boss were expressed in S2 cells. Immunoprecipitates of PAPLA1 (V5) contained Boss (Flag) but not ceramidase (CDase), a glycosylated and secreted protein. CE, crude extract; IP, immunoprecipitation.

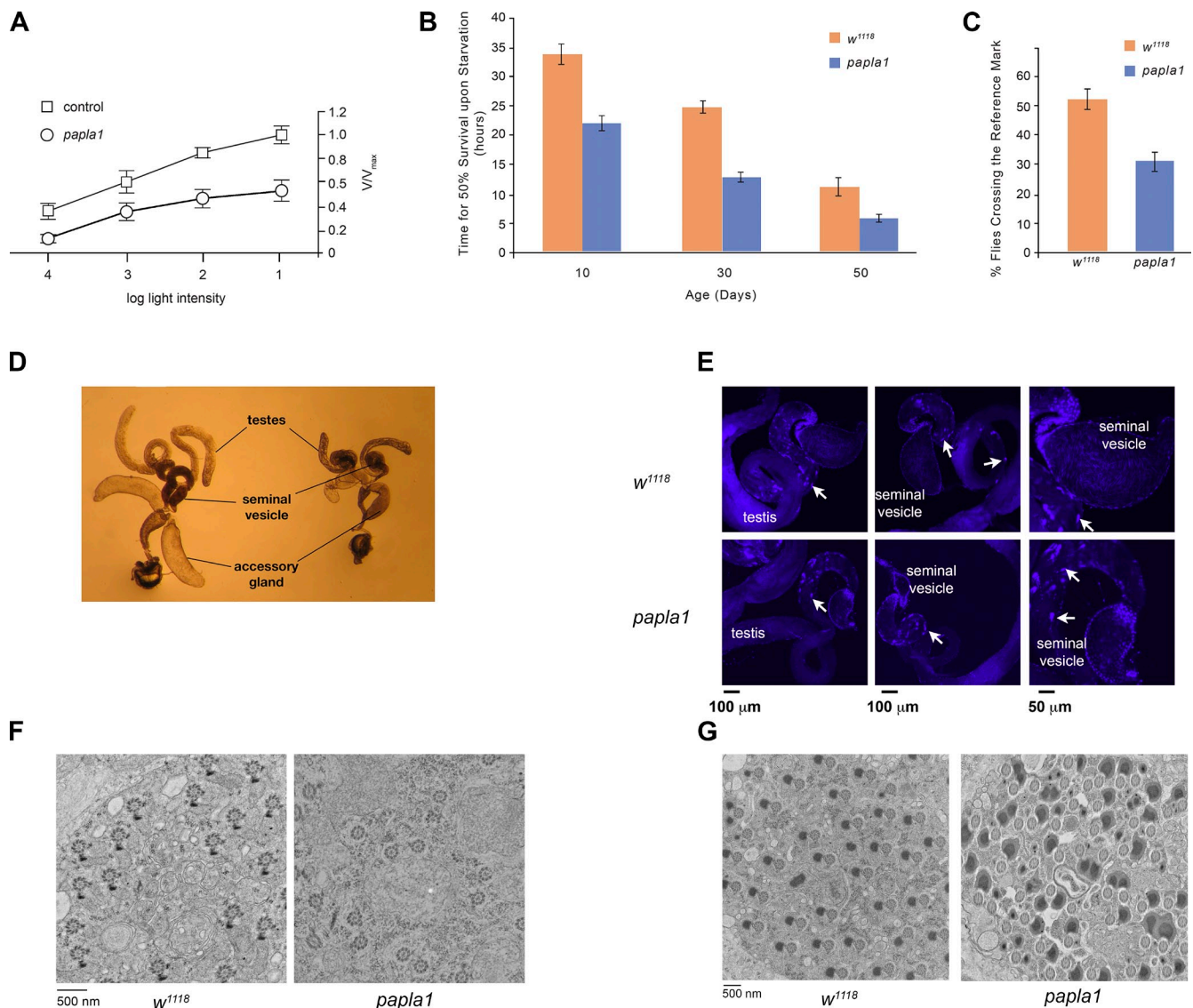


**Figure 6. *papla1* mutants show decreased light sensitivity and increased susceptibility to starvation and are male sterile.** (A) ERG analysis of control and *papla1* mutant flies. The light was attenuated through a series of neutral density filters in which 1 = no filter, 2 = 10% transmitted light, 3 = 1% transmitted light, and 4 = 0.1% transmitted light. A total of six control and mutant flies were examined. (B) *papla1* mutant flies succumb to starvation faster than controls. The mean time for 50% survival during starvation was plotted for each age group of the control and mutant flies ( $n = 6$ ). (C) *papla1* mutant flies display decreased locomotor activity ( $n = 7$ ). (D–G) *papla1* mutant flies are male sterile as a result of defective spermatogenesis. (D) The *papla1* mutants have smaller testis compared with the controls. (E) DAPI of the male sex organs. Arrows, elongated spermatid bundles. (F and G) Electron micrograph of early spermatid bundles (F) and mature spermatid bundles before individualization of the sperms (G). The error bars indicate standard error of the means.

and protection to Rh1. Although ectopically localized proteins could be unstable and degraded, the glycosylated Rh1 has been reported to undergo slightly faster endocytosis and degradation (Cao et al., 2011). This could also contribute to the low levels of GPCRs observed in the *papla1* mutant. N-glycan addition and alterations function as tags that aid in quality control of the protein as it folds, traffics, and matures along the secretory pathway. Any defect in one of these processes alters the glycosylation state of the protein and subjects it to degradation or reprocessing. The failure to traverse through the Golgi complex does not abrogate the anterograde transport of Rh1 completely in the *papla1* mutant because we still find that a small fraction of the higher glycosylated form of Rh1 localizes to the rhabdomere. This could result from the ability of InaD and other

proteins to concentrate the randomly targeted Rh1 to the rhabdomere (Tsunoda et al., 1997; Li and Montell, 2000). The Golgi complex has a very important role in ensuring the processing, sorting, and finally, targeting of newly synthesized proteins to the correct destination. The absence of PAPLA1 has tangible deleterious effects on the flies. First, in the eyes, we see a steady decrease in the levels of Rh1 protein which leads to a substantial decrease in the sensitivity of these flies to light stimuli. Another significant phenotype of the *papla1* mutants is that they are male sterile. A point to note is that PAPLA1 function in spermatogenesis is distinct from its function in Rh1 or Boss trafficking. The phospholipase activity of PAPLA1 is critical for spermatogenesis and individualization of sperms in *Drosophila*, whereas it is not required for the vesicular transport function of the protein.

Recently, it was reported that mutations in the human DDHD1 and DDHD2 proteins cause recessive hereditary spastic paraplegia (Schuurs-Hoeijmakers et al., 2012; Tesson et al., 2012; Fink, 2013; Gonzalez et al., 2013). Those studies were not able to identify specific defects in protein transport but rather indicated a deficiency in synaptic transmission. *papla1* mutants do not show a catastrophic decrease in the levels of the proteins (e.g., Rh1 or Boss) that are compromised in its absence. Rather, the steady decline in Rh1 in the *papla1* mutant leads to a slow deterioration in photoreceptor function. Likewise, we see a slow deterioration in the vitality of the flies with regard to mobility and starvation responses. A similar loss of critical proteins could explain the onset and progress of hereditary spastic paraplegic in patients with mutations in DDHD1 and DDHD2 proteins.

## Materials and methods

### Fly stocks and husbandry

*Drosophila* stocks (*dmppe* [13884]; *w<sup>1118</sup>* [3605]; and *cn*, *bw* [264]) were obtained from the Bloomington Stock Center. hs-Rh1-1D4 (a transgenic fly in which Rh1 cDNA is translationally fused to a 12-amino acid 1D4 epitope at the C terminus and is driven by an Hsp70 promoter), *ninaA<sup>269</sup>*, and *ninaA<sup>1</sup>* were obtained from C. Zuker (Columbia University, New York, NY). *Drosophila* were raised on standard maize meal agar and maintained at 25°C unless otherwise mentioned. UAS-PAPLA1 flies were generated using standard molecular biology techniques. The 31-kb genomic rescue construct was cloned into the P[acman] ampicillin vector using recombineering methods as described previously (Venken et al., 2006). The V5N-PAPLA1 and the active site mutant genomic constructs were generated using recombineering-based *galK* selection and counter selection using the 31-kb genomic rescue construct (Warming et al., 2005).

### Genetic screen to isolate *papla1*-null mutants

The PAPLA1 knockout line (*papla1*) was generated by ends-out homologous recombination (Gong and Golic, 2003). The targeting vector was designed to delete exons 2–6. Using this strategy, 5,756 bp of  $\Delta$ 18,761–24,516 of the PAPLA1 gene was deleted. pW25 (Drosophila Genomics Resource Center) was used to make donor constructs. Primers P1 and P2 were used to amplify the upstream homology arm for *papla1*. P3 and P4 were used for the downstream arm. The transgenic flies carrying the donor constructs were crossed to flies expressing Flippase and I-SceI and then used. G1 female progeny were crossed to males expressing Flippase constitutively, and 1,000 lines were generated. In G2 generation, flies were screened for red-eyed progeny. These flies with potential targeted mutants were crossed to appropriate flies to establish stocks. The targeted alleles were confirmed by PCR-based techniques. The mutant flies have red eyes with the *white<sup>+</sup>* gene. The *white<sup>+</sup>* was removed by crossing to Cre recombinase-expressing flies. Finally, the white-eyed mutants were confirmed by PCR using primers P5 and P6. The predicted length of PCR products is 362 bp in *papla1* and 6,442 bp in *w<sup>1118</sup>* (see Table 1 for primer sequences).

### Generation of rescue constructs by homologous recombination

To generate transgenic flies expressing the PAPLA1 protein at the endogenous level, three P[acman]-based constructs were generated using recombineering and recombineering-based *galK* selection (Warming et al., 2005; Venken et al., 2006): (1) P[acman]-PAPLA1, by direct retrieval of PAPLA1 genomic DNA plus the promoter region from bacterial artificial chromosome (BAC) into the P[acman] vector; (2) P[acman]-V5-N-PAPLA1, P[acman]-PAPLA1 with a V5 tag at the N termini; and (3)  $\Delta$ 1,682–1,686-PAPLA1, the active site mutant.

**P[acman]-PAPLA1.** The left homology arm (primers P7 and P8) and right homology arm (primers P9 and P10) were first inserted into the multiple cloning site of P[acman] (1245; Drosophila Genomics Resource Center). The constructs were linearized with BamHI and transformed into recombineering bacteria DY380 containing PAPLA1 BAC. We retrieved 30,484 bp of DNA from BAC into the P[acman] constructs by homologous recombination. The final constructs were confirmed by PCR. Primers P11 and P12 were used for amplifying upstream junctions, and P13 and P14 were used for downstream junctions.

**P[acman]-V5-N-PAPLA1.** This construct integrates 42 bp of the V5 epitope exactly before the PAPLA1 start codon and was engineered using *galK*-based positive-negative selection (Warming et al., 2005; Venken et al., 2006). We designed *galK* primers (P15 and P16) with a 75-bp homology to an area flanking the desired site. The 3' end of these primers binds to the *galK* cassette. The purified PCR products were transformed into SW102 cells containing the construct P[acman]-PAPLA1. The correct recombinants grow on M63 minimal media plates with galactose as the carbon source, and thus, the *galK*-positive colonies can be selected. Single red colonies were picked, and PCR (P17 and P18) was performed to confirm the integration of the *galK* cassette at the desired site. The predicted PCR product size was 420 bp. Primers P19 and P20 were used to generate a targeting construct containing the V5 epitope and 80 bp of homology to replace the *galK* cassette. The PCR product was introduced into the confirmed *galK*-positive SW102 cells, and the targeting sequence replaced the *galK* cassette by homologous recombination. The correct recombinant grew on M63 plates containing biotin and 2-deoxy-galactose and ampicillin with glycerol as a carbon source, and thus, we selected *galK*-negative colonies. The correct colonies were confirmed by PCR using primers P21 and P22, and the predicted PCR product size is 311 bp. Finally, the V5 epitope sequence and site were confirmed by sequencing.

**Δ1,682–1,686-PAPLA1.** This construct deletes 15 bp of internal sequence coding for amino acids 1,682–1,686 in the 31-kb P[acman]-PAPLA1. We designed *galK* primers (P23 and P24) with 76-bp homology to the area flanking the desired site. The 3' end of these primers binds to the *galK* cassette. Subsequent manipulations were similar to the procedure described in the preceding paragraph. Single red colonies were picked to perform PCR (P25 and P26) and confirm the integration of *galK* cassette at the desired site. Primers P27 and P28 were used to generate a targeting vector containing 106 bp of homology to replace the *galK* cassette. The correct recombinant grew on M63 plates containing biotin and 2-deoxy-galactose and ampicillin with glycerol as a carbon source, and thus, we selected *galK*-negative colonies. The correct colonies were confirmed by sequencing.

The UAS-PAPLA1 was cloned by using LD21067 (1622894; Drosophila Genomic Resource Center) as a template to PCR of the full-length cDNA cloned into the EcoR1–Kpn1 site of the pUAST vector. Glass multi-meric reporter-Gal4 was used as a driver for overexpression of the protein in the photoreceptor cells.

For UAS-NinaA cloning, the NinaA gene was obtained by reverse transcribing the gene from total RNA prepared from wild-type control fly heads and cloned into the EcoR1–Not1 site of the pUAST vector. Transgenic flies were generated from a clone that was confirmed by sequencing.

### Dissection and staining of testis

100  $\mu$ l of cold PBS was pipetted onto the microscope slide (VWR International). A male adult fly is placed onto the slide, and the bottom of the fly body was dissected out with the forceps under a microscope. The gut was removed, and the whole testes together with seminal vesicles and accessory glands were set aside. The testis was washed with PBS containing 0.1% Triton X-100 three times in an Eppendorf tube. The testis was fixed with 4% formaldehyde solution for 30 min at room temperature. The testis was mounted on microscope slides with mounting medium containing DAPI, and images were captured under a confocal microscope (LSM 510; Carl Zeiss).

### Electron microscopy

For all electron microscopic experiments, unless otherwise specified, 7-d-old flies grown at 25°C were decapitated under anesthesia, and their heads were dissected and fixed in a solution sodium cacodylate buffer containing 2% glutaraldehyde and 4% formaldehyde. They were then postfixed in 1% osmium tetroxide, dehydrated, and embedded in epoxy resin (Embed 812), and thin sections were cut (Acharya et al., 2003).

### Immunohistochemistry

PAPLA1 staining was performed on *papla1*-null flies rescued by the V5-N-PAPLA1 genomic construct. In brief, tissues were dissected from adult flies and third instar wandering larvae, fixed with 4% paraformaldehyde, and blocked in PBS containing 0.2% Triton X-100 and 5% normal goat serum for 2 h. The tissues were stained with primary antibody in blocking buffer overnight at 4°C, washed with PBS, and stained with secondary antibody in blocking buffer at room temperature. Tissues were washed, and coverslips were mounted using Vectashield. The *Drosophila* whole-mount retinal staining from adult flies was performed as previously described (Walther and Pichaud, 2006). In brief, fly heads were bisected under anesthesia; the heads were then dissected in 4% paraformaldehyde in PBS.

Table 1. Primer sequences used in this study

Primers	Sequences (5' → 3')
P1	TCATCGTACCGCATCAAACGGGCATCGAATTGG
P2	GCTCGGGCGCCCTGATGCCATTGTTATAGTTGGAGAT
P3	TATATAGGTACCGAGGATCAGGACGAGAGTTC
P4	TATATAGGGCCGCCACTCACCACAAAC
P5	TGCGGCTATCGCTGTTAG
P6	GTTTCAAGATGAACCTGCCA
P7	AATTGGCGCCCTAAACCGCAGTCATGTGCTGCC
P8	ATATGGATCCGTCAGCGCAGGCACGGAAAAGCGTC
P9	ACGAGAGCTGTTGGATCCAACG
P10	CGCGTTAATTAAAGAAGCGCTCCAAATAACCTC
P11	TTTAAACCTCGAGCGGTCCGTTATC
P12	GCTCGCACACCGTGATTTTCAAG
P13	AATCAGCACAGACAGCCAGGTG
P14	CTAAAGGGAAACAAAAGCTGGTAC
P15	GCAACTGTGCACTTGGCACACATCTCATCGAGTTAGCCAATTAAAGCTCCAGATCGGCCGTAATATGCCGTTGACAATTAAATCATCGG CATAG
P16	AAGCGGATTTAAACGACACCGCTCTGGTTGCGTTGTTACCGGAGCGGACACGTACCTTCGATCTTCGACTCAGCACTGCTGCT CCTTG
P17	CGGCTGTATCGTCGGCTGATC
P18	GCAGCGAGCAACAGGTGACC
P19	CTAAGGCAACTGTGCACTTGGCACACATCTCATCGAGTTAGCCAATTAAAGCTCCAGATCGGCCGTAATATGGTAAGCCTATCCCTAAC CCTCTCCTCGTCTCGATTCTACG
P20	AAGCGGATTTAAACGACACCGCTCTGGTTGCGTTGTTACCGGAGCGGACACGTACCTTCGATCTTCGACGTTAGGATCGAGACCGAG GAGAGGGTTAGGGATAGGCTTAC
P21	CCTATCCCTAACCTCTCCG
P22	GCAGCGAGCAACAGGTGACC
P23	GGCAGATCGCTTAACGATGCTACCTGAAGTACCGAATCGGCACCCGAATTCAATGGGGAGTTCGCTGGCACCTGTTGACAATTAAATCAT CGGA
P24	AAGTTTACTCACTTATTCTCTTCGCTTCCGTTGAGCGTTCTGATGGCACAATAATCGAATAGGATTAGGATCAGCACTGCTGCT CCTT
P25	GCATCGACGAAAGCTGAATCC
P26	TTTCAGACTCATGATCTGCCCTC
P27	GAAATACTGTCAAAGATCATGAACACGGTGGCAGATCGCCTAACGATGTCTACCTGAAGTACCGAATCGGCACCCGAATTCAATGGGGAG TTTCGCTGGCA
P28	AATGGTTTATTAAATCGCTAAAGTTTACTCACTTATTCTCTTCGCTTCCGTTGAGCGTTCTGATGGCACAATAATCGAATAGGATTAG GGATGCCAGCGAAACTCCCCATTGAATT

The tissues surrounding each compound eye were removed using forceps, and the lens material surrounding each eye was carefully removed from the eye. The dissected eyes were pooled and processed for antibody staining. The antibody to Lava lamp (rabbit) was a gift from J. Sisson (University of Texas, Austin, TX) and C. Fields (Harvard Medical School, Boston, MA). The rabbit antibody to NinaC was a gift from N. Colley (University of Wisconsin, Madison, WI). Anti-V5 mouse monoclonal (1:200; Invitrogen) and polyclonal (rabbit) antibodies (1:200; Sigma-Aldrich) were used in immunolocalization experiments. The anti-Golgi mouse monoclonal antibody (7H6D7C2; 1:200) was obtained from EMD Millipore. The rhodopsin mouse monoclonal antibody (4C5) was obtained from Developmental Studies Hybridoma Bank. The RHO-1D4 mouse monoclonal antibody (1:25) was obtained from The University of British Columbia (Vancouver, British Columbia, Canada). Alexa Fluor dye-conjugated (488 nm, 564 nm, and 647 nm) secondary antibodies were used for immunolocalization in fluorescence experiments. DAPI was used for staining the nuclei. Retinal immunolocalization data were acquired on a confocal microscope (LSM 510) using a 60 $\times$  objective. For quantification of colocalization of Sec23 and PAPLA1, six areas from three confocal sections of the accessory glands with larger immunostained structures were examined. Individual green, blue, and overlapping structures were counted, and the percentage of overlap was calculated for each of the areas. The images were processed in Photoshop (Adobe) for arrangement, cropping, and presentation.

#### SR-SIM

The images were acquired on a demonstration model of ELYRA S1 SR-SIM and an electron-multiplying charge-coupled device camera (iXon EM 885;

Andor Technology) with an 8- $\mu$ m pixel size. Images were acquired with a Plan Apochromat 100 $\times$ , 1.40 NA oil immersion objective, and the image pixel size of the raw data was 50 nm. Images were acquired with five or three grid rotations. Raw images were reconstructed and processed using the Zen 2011 software (Carl Zeiss) with a structured illumination microscope analysis module to generate the final images. The channel alignment reference image was based on a multicolor bead slide (TetraSpeck; Life Technologies). The colors were aligned to the channel using an affine fit that corrected for axial shift, lateral shift, rotation, and spine. Colors were aligned to one structured illumination microscope pixel accuracy (25 nm). The images obtained were then processed in Photoshop for cropping, arrangement, and presentation.

#### Western analysis

Fly heads were dissected from 3-d-old flies (unless otherwise specified), homogenized in sample buffer, boiled, and subjected to SDS-PAGE and Western analysis. For detection of Rh1 and other proteins detected in the same blot, the samples were incubated at 37°C for 40 min and then subjected to SDS-PAGE and Western blotting. Antibodies to Rh1 (rabbit polyclonal), NinaA (rabbit), and Trp (rabbit) were gifts from C. Zuker, antibody to NinaC (rabbit) was a gift from C. Montell (Johns Hopkins University, Baltimore, MD), and the rhodopsin (4C5), neuroglian, and the tubulin (E7) mouse monoclonal antibodies were obtained from the Developmental Studies Hybridoma Bank. The guinea pig anticontactin antibody was a gift from M. Bhat (The University of Texas, Austin, TX). The Boss monoclonal antibody was a gift from L. Zipursky (University of California, Los Angeles, Los Angeles, CA).

### PNGase F treatment of Rh1 or Boss

15 *w<sup>1118</sup>* and 15 *papla1* mutant heads were collected and homogenized initially in 100  $\mu$ l PBS, and then, the volume was adjusted to 1 ml, mixed well, and centrifuged at 1,000  $\times$ g to remove debris. The supernatant was centrifuged at 20,000  $\times$ g to pellet membranes. The membrane pellet was resuspended in 90  $\mu$ l H<sub>2</sub>O, and 10  $\mu$ l of 10x denaturing buffer (5% SDS and 400 mM DTT) was added, mixed by pipetting, and allowed to solubilize at 4°C for 30 min. The supernatant was centrifuged at 10,000  $\times$ g to remove insoluble proteins. To 10  $\mu$ l supernatant, 2  $\mu$ l of 10% NP-40 and 2  $\mu$ l of 10x reaction buffer (500 mM sodium phosphate, pH 7.5) were added, and the volume was adjusted to 19  $\mu$ l and mixed gently. Finally 1  $\mu$ l PNGase F (500,000 U/ml) was added, mixed, and incubated at 37°C for 1 h. The reaction was terminated by adding 2x SDS loading dye, and the products were run on a 13% SDS-PAGE gel for Rh1 and a 10% SDS-PAGE gel for Boss (for the latter, the gels were overrun to resolve better). Subsequently, proteins were transferred to polyvinylidene fluoride membrane, and Western blotting was performed with mouse Rh1 or Boss antibodies.

### Immunoprecipitation of Rh1

100 *w<sup>1118</sup>* and *papla1* heads were homogenized initially with 200  $\mu$ l PBS, and the volume was adjusted to 1.5 ml and mixed well. The lysates were centrifuged at 1,000  $\times$ g to remove debris. Supernatant was centrifuged at 20,000  $\times$ g for 1 h, and membrane pellet was resuspended in solubilization buffer (50 mM Tris-HCl, pH 7.4, 300 mM NaCl, 5 mM EDTA, and 1% n-dodecyl maltoside). The membrane was allowed to solubilize at 4°C for 3–4 h on a rocker followed by centrifugation at 10,000  $\times$ g for 10 min to remove detergent-insoluble proteins. To the supernatant, 5  $\mu$ l Rh1 antibody (ascites of 5–10  $\mu$ g) was added and mixed, and 50  $\mu$ l protein G beads was added and left on a rocker overnight at 4°C. Beads were collected by centrifugation (1,000  $\times$ g) and washed three times with solubilization buffer, two times with PBST (PBS with Tween), and finally, two times with PBS (3–5 min each). After PBS wash, the entire buffer was removed by pipetting, and 20  $\mu$ l elution buffer was added, gently mixed, and incubated on ice for 5 min. The eluate was collected by pipetting and mixed with 10  $\mu$ l SDS loading dye. The sample was analyzed on 13% SDS-PAGE (gel was overrun until a 29-kD marker band reached near the end of the gel) and silver stained.

### Coimmunoprecipitation of hs-Rh1-1D4 and V5N-PAPLA1 flies

Transgenic hs-Rh1-1D4; V5N-PAPLA1 flies (eclosed in <24 h) were incubated for 1 h at 37°C and recovered for 3 h at 25°C. Heads were decapitated (600) and homogenized in 3 ml of buffer A (20 mM Tris-HCl, pH 7.5, 50 mM NaCl, 2.5 mM EDTA, and protease inhibitors). The homogenate was centrifuged at 10,000  $\times$ g for 10 min to remove debris and rhabdomeric membranes. The supernatant was centrifuged at 200,000  $\times$ g for 1 h with a rotor (MLS 130K; Beckman Coulter), and the microsome pellet was resuspended in 1 ml of buffer B (20 mM Tris-HCl, pH 7.5, 50 mM NaCl, 2.5 mM EDTA, 0.1% sodium dodecyl maltoside, and protease inhibitors) and incubated at 4°C for 2 h. The insoluble proteins and membranes were removed by centrifugation at 10,000  $\times$ g for 10 min. The supernatant was incubated with 30  $\mu$ l protein G beads coupled to IgG- or V5 epitope-specific antibodies (4  $\mu$ g) for 3 h at 4°C. Beads were collected by centrifugation at 100  $\times$ g for 3 min and washed three to five times with buffer B, and proteins were eluted by SDS loading buffer. The samples were analyzed by Western blotting with appropriate antibodies. The blots were probed for contactin, a glycosylated glycosylphosphatidylinositol-anchored membrane protein apparently unaffected in the *papla1* mutant, and CERT (ceramide transfer protein), which localizes to the ER and Golgi complex, and both served as negative controls (Faivre-Sarrailh et al., 2004; Rao et al., 2007).

### Immunoprecipitation of PAPLA1 and Western blots with Sec23

About 100 V5N-PAPLA1 transgenic fly heads (<1 d old) were homogenized in 1 ml PBS containing 0.4% NP-40 and 2.5 mM EDTA (solubilization) and allowed to solubilize for 2–4 h at 4°C on a rocker. The lysates were centrifuged at 10,000  $\times$ g to remove the insoluble fraction. To the supernatant, 20  $\mu$ l protein G beads was added and incubated on a rocker at 4°C for 1 h. The beads were removed by centrifugation, and the supernatant was collected in a fresh tube. To the supernatant, 4  $\mu$ g of mouse V5 antibody (Invitrogen) conjugated to 20  $\mu$ l protein G beads was added and incubated at 4°C for 3 h on a rocker. Beads were collected by centrifugation and washed three times with solubilization buffer (10 min each). Finally, the entire buffer was removed from the beads, and 2x SDS loading dye was added to elute proteins. Eluted proteins were boiled to

denature and loaded on 8 or 10% SDS-PAGE. Proteins were transferred to a polyvinylidene fluoride membrane, and standard Western blotting was performed using a rabbit COPII antibody (Thermo Fisher Scientific).

### Cell culture

*Drosophila* S2 cells and stable S2 cells were grown at 25°C in Schneider's *Drosophila* medium (Invitrogen) supplemented with L-glutamine, 10% FBS, and penicillin-streptomycin. Stable S2 cells expressing a V5-tagged PAPLA1 under blasticidin (A.G. Scientific, Inc.) selection and Flag-tagged Sec23 or Sec31 under hygromycin (Roche) selection were used in the experiments.

### Immunoprecipitation of PAPLA1 and interacting proteins in S2 cells

Antibodies were conjugated to Dynabeads protein G (Invitrogen) by adding 4  $\mu$ g of mouse IgG, anti-V5, or anti-Flag antibodies diluted in 400  $\mu$ l PBS with 0.02% Tween 20 to 30  $\mu$ l Dynabeads protein G and rotated for 2 h at 4°C. Beads were washed in PBS with 0.02% Tween 20. Cells were plated at 10<sup>6</sup> in a 10-cm dish. Cells were induced with CuSO<sub>4</sub> at a final concentration of 500  $\mu$ M CuSO<sub>4</sub>. After 24 h, cells were harvested, washed with cold PBS, suspended with cold 1.5 ml lysis buffer (PBS, 5 mM EDTA, and 0.6% NP-40) containing protein inhibitors, and rotated for 2 h at 4°C. The lysate was centrifuged at 10,000  $\times$ g for 10 min to remove the cell debris. 500  $\mu$ l supernatant was added to each conjugated Dynabeads protein G and rotated for 3 h at 4°C. The beads were washed five times with lysis buffer, and the samples were eluted in 50  $\mu$ l SDS sample buffer. The sample was loaded on SDS-PAGE gels, and Western blotting was performed with appropriate antibodies. For Boss immunoprecipitation, V5 epitope-tagged PAPLA1 (pMT/V5; Invitrogen) protein and Flag-tagged Boss protein under an actin promoter (modified pAc5.1; Invitrogen) were transfected into S2 cells. 24 h after transfection, PAPLA1 was induced with copper sulfate, and immunoprecipitation and Western blot analysis were performed as described earlier in this paragraph. For Boss, ceramidase, a glycosylated and secreted protein, was used as a negative control (Acharya et al., 2008).

### Immunoprecipitation of PAPLA1 and the deletion mutant for phospholipase A1 assay

The C-terminally V5 epitope-tagged wild-type PAPLA1 and active site mutant PAPLA1 were stably expressed in S2 cells under blasticidin selection. Induction of protein expression and immunoprecipitation was performed as described for PAPLA1 and COPII coimmunoprecipitation, except protein G-Sepharose beads were used for immuno-pull-down. Protein G beads containing equal amounts of wild-type and mutant proteins were used for the assay.

### Electroretinography

ERGs were recorded as described previously (Gavin et al., 2007). In brief, flies were anesthetized with carbon dioxide and immobilized on a rotating disc using molten myristic acid (Akonchem). The voltage changes were recorded with a SigmaGel (Parker Laboratories, Inc.)-filled electrode that was placed in contact with the surface of the eye, whereas a second similarly gel-filled electrode was impaled into the thorax. A halogen lamp controlled by a shutter (model T132; Uniblitz) was used to generate light signals. All light treatments, unless otherwise stated, were performed using a 580-nm filter. The light was attenuated through neutral density filters (Oriel Instruments). An amplifier (DAM50; World Precision Instruments) was used to amplify the voltage changes recorded using Powerlab 4/30 (ADI Instruments) and analyzed with the help of Chart 5 software (ADI Instruments).

### Negative geotaxis experiments

The negative geotaxis assay was performed as described previously with some changes (Rao et al., 2007). 30-d-old flies maintained on a normal diet were taken in an empty vial (10-cm vials with 15 flies in each). The vials were tapped twice on the table to initiate the flies, and the number of flies that crossed a reference mark (7 cm from the bottom of the vial) in 30 s was counted. The procedure was repeated for seven trials, and between trials, the flies were allowed to rest for 30 s.

### Glycan analysis

In-gel tryptic digestions of Rh1 immunoprecipitated from wild-type and *papla1* mutant heads were based on previously published procedures (Küster et al., 1997; Chill et al., 2009). In brief, silver-stained SDS gel pieces were cut into small pieces and washed in a solution containing 40 mM ammonium bicarbonate (AmBic) for 10 min and were then dehydrated with 100% acetonitrile for ~10 min. This procedure was repeated until the gel turned white. Subsequently, the dehydrated gel pieces were reswollen for an hour at 55°C in a solution containing 10 mM DTT and 40 mM AmBic. After cooling to room temperature, this solution was replaced with

a solution containing 55 mM iodoacetamide and incubated in the dark for 45 min. Subsequently, the gel pieces were washed with 40 mM AmBic and dehydrated (10 min) in acetonitrile. The gel pieces were rehydrated on ice in digestion solution (containing 50 µg trypsin and chymotrypsin in 1 ml of 40-mM AmBic) for 45 min and then incubated overnight at 37°C. The following morning, the incubation solution was collected, and gel pieces were serially extracted with 20, 50, and 80% acetonitrile (all in 5% aqueous formic acid). The original incubation solution and all subsequent extracts were combined, dried, and subjected to chromatography (C18 Sep-Pak; Waters) to separate peptides and glycopeptides (Aoki et al., 2007). PNGase F digestion was performed to release the glycans from the glycopeptides and was permethylated for nanospray ionization MS. An ion trap instrument (NSI-LTQ Orbitrap Discovery; Thermo Fisher Scientific) was used for identification as previously described (Aoki et al., 2007). After permethylation, dried glycans were dissolved in 1 mM NaOH in 50% methanol and directly infused into the instrument at a syringe flow rate of 0.40–0.60 µl/min. For fragmentation by collision-induced dissociation in MS/MS and MS<sup>n</sup> modes, 40% collision energy was applied. The total ion mapping functionality of the XCalibur software package (version 2.0; Thermo Fisher Scientific) was used to detect and quantify the prevalence of individual glycans in the total glycan profile. Most permethylated oligosaccharides were identified as singly, doubly, and triply charged species by nanospray ionization–MS. Peak intensities for all charge states of a given glycan with mass per charge <2,000 were summed together for quantification.

#### Online supplemental material

Fig. S1 shows that PAPLA1 colocalizes with COPII and not Golgi components, that it interacts with Sec23 and Sec31 in S2 cells, and that although Rh1 is affected in the *papla1* mutant, other phototransduction components are not compromised. Fig. S2 shows that steady-state levels and apparent molecular masses of GPCRs Rh1 and Boss are compromised in *papla1* mutants, whereas other glycosylated proteins, such as contactin and neuroglian, are not affected. Fig. S3 shows that Rh1 is aberrantly localized in the *papla1* mutant, that the N-terminal V5-tagged PAPLA1 genomic construct rescues transport defect in the *papla1* mutant, that the active site mutant protein is catalytically inactive, and that the active site mutant transgenic construct is able to rescue Rh1 maturation in *papla1* mutants. Fig. S4 shows a defect in Rh1 transport in *papla1* mutants using a pulse–chase paradigm and immunofluorescence experiments. Fig. S5 demonstrates that the Rh1 is mostly retained in the ER in *papla1* mutants. Online supplemental material is available at <http://www.jcb.org/cgi/content/full/jcb.201405020/DC1>.

We thank Dr. Charles Zuker for antibodies (Rh1, NorpA, Trp, and NinaA) and flies (*ninaA*<sup>209</sup>, *ninaA*<sup>1</sup>, and hs-Rh1-1D4), Dr. Larry Zipursky for the Boss monoclonal antibody, Dr. John Sisson (late) and Dr. Christine Field for the lava lamp antibody, Dr. Craig Montell for the NinaC antibody, Dr. Nansi Colley for the NinaC antibody, Dr. Manzoor Bhat for the contactin antibody, the Bloomington Stock Center for fly stocks and reagents, and the Hybridoma Bank for Rh1, neuroglian, and tubulin antibodies. We thank Stephen Lockett and Kim Peifley from the National Cancer Institute confocal facility and Bryant Chhun from Carl Zeiss for help with confocal and superresolution microscopy. We thank Dr. Shyam Sharan for comments on the manuscript.

This study was funded by the intramural division of the National Cancer Institute, National Institutes of Health (Division of Health and Human Services). M. Tiemeyer acknowledges the support from National Institutes of Health (co-equal principal investigator; P41GM103490) for MS. U. Acharya is supported by the National Institutes of Health (RO1EY016469).

The authors declare no competing financial interests.

Submitted: 6 May 2014

Accepted: 2 June 2014

## References

Acharya, J.K., U. Dasgupta, S.S. Rawat, C. Yuan, P.D. Sanxaridis, I. Yonamine, P. Karim, K. Nagashima, M.H. Brodsky, S. Tsunoda, and U. Acharya. 2008. Cell-nonautonomous function of ceramidase in photoreceptor homeostasis. *Neuron*. 57:69–79. <http://dx.doi.org/10.1016/j.neuron.2007.10.041>

Acharya, U., S. Patel, E. Koundakjian, K. Nagashima, X. Han, and J.K. Acharya. 2003. Modulating sphingolipid biosynthetic pathway rescues photoreceptor degeneration. *Science*. 299:1740–1743. <http://dx.doi.org/10.1126/science.1080549>

Aoki, K., M. Perlman, J.M. Lim, R. Cantu, L. Wells, and M. Tiemeyer. 2007. Dynamic developmental elaboration of N-linked glycan complexity in the *Drosophila melanogaster* embryo. *J. Biol. Chem.* 282:9127–9142. <http://dx.doi.org/10.1074/jbc.M606711200>

Arimitsu, N., T. Kogure, T. Baba, K. Nakao, H. Hamamoto, K. Sekimizu, A. Yamamoto, H. Nakanishi, R. Taguchi, M. Tagaya, and K. Tani. 2011. p125/Sec23-interacting protein (Sec23ip) is required for spermiogenesis. *FEBS Lett.* 585:2171–2176. <http://dx.doi.org/10.1016/j.febslet.2011.05.050>

Balch, W.E., J.M. McCaffery, H. Plutner, and M.G. Farquhar. 1994. Vesicular stomatitis virus glycoprotein is sorted and concentrated during export from the endoplasmic reticulum. *Cell*. 76:841–852. [http://dx.doi.org/10.1016/0092-8674\(94\)90359-X](http://dx.doi.org/10.1016/0092-8674(94)90359-X)

Barlowe, C.K., and E.A. Miller. 2013. Secretory protein biogenesis and traffic in the early secretory pathway. *Genetics*. 193:383–410. <http://dx.doi.org/10.1534/genetics.112.142810>

Belden, W.J., and C. Barlowe. 2001. Role of Erv29p in collecting soluble secretory proteins into ER-derived transport vesicles. *Science*. 294:1528–1531. <http://dx.doi.org/10.1126/science.1065224>

Bieber, A.J., P.M. Snow, M. Hortsch, N.H. Patel, J.R. Jacobs, Z.R. Traquina, J. Schilling, and C.S. Goodman. 1989. *Drosophila* neuroglan: a member of the immunoglobulin superfamily with extensive homology to the vertebrate neural adhesion molecule L1. *Cell*. 59:447–460. [http://dx.doi.org/10.1016/0092-8674\(89\)90029-9](http://dx.doi.org/10.1016/0092-8674(89)90029-9)

Cao, J., Y. Li, W. Xia, K. Reddig, W. Hu, W. Xie, H.S. Li, and J. Han. 2011. A *Drosophila* metallophosphoesterase mediates deglycosylation of rhodopsin. *EMBO J.* 30:3701–3713. <http://dx.doi.org/10.1038/embj.2011.254>

Chill, L., L. Trinh, P. Azadi, M. Ishihara, R. Sonon, E. Karnaukhova, Y. Ophir, B. Golding, and J. Shiloach. 2009. Production, purification, and characterization of human alpha1 proteinase inhibitor from *Aspergillus niger*. *Biotechnol. Bioeng.* 102:828–844. <http://dx.doi.org/10.1002/bit.22099>

Colley, N.J., E.K. Baker, M.A. Stammes, and C.S. Zuker. 1991. The cyclophilin homolog ninaA is required in the secretory pathway. *Cell*. 67:255–263. [http://dx.doi.org/10.1016/0092-8674\(91\)90177-Z](http://dx.doi.org/10.1016/0092-8674(91)90177-Z)

Colley, N.J., J.A. Cassill, E.K. Baker, and C.S. Zuker. 1995. Defective intracellular transport is the molecular basis of rhodopsin-dependent dominant retinal degeneration. *Proc. Natl. Acad. Sci. USA*. 92:3070–3074. <http://dx.doi.org/10.1073/pnas.92.7.3070>

Davis, R.C., G. Stahnke, H. Wong, M.H. Doolittle, D. Ameis, H. Will, and M.C. Schotz. 1990. Hepatic lipase: site-directed mutagenesis of a serine residue important for catalytic activity. *J. Biol. Chem.* 265:6291–6295.

Derewenda, Z.S. 1994. Structure and function of lipases. *Adv. Protein Chem.* 45:1–52. [http://dx.doi.org/10.1016/S0065-3233\(08\)60637-3](http://dx.doi.org/10.1016/S0065-3233(08)60637-3)

Emmerich, J., O.U. Beg, J. Peterson, L. Previato, J.D. Brunzell, H.B. Brewer Jr., and S. Santamarina-Fojo. 1992. Human lipoprotein lipase. Analysis of the catalytic triad by site-directed mutagenesis of Ser-132, Asp-156, and His-241. *J. Biol. Chem.* 267:4161–4165.

Faivre-Sarrailh, C., S. Banerjee, J. Li, M. Hortsch, M. Laval, and M.A. Bhat. 2004. *Drosophila* contactin, a homolog of vertebrate contactin, is required for septate junction organization and paracellular barrier function. *Development*. 131:4931–4942. <http://dx.doi.org/10.1242/dev.01372>

Fink, J.K. 2013. Hereditary spastic paraparesis: clinico-pathologic features and emerging molecular mechanisms. *Acta Neuropathol.* 126:307–328. <http://dx.doi.org/10.1007/s00401-013-1115-8>

Fromme, J.C., L. Orci, and R. Schekman. 2008. Coordination of COPII vesicle trafficking by Sec23. *Trends Cell Biol.* 18:330–336. <http://dx.doi.org/10.1016/j.tcb.2008.04.006>

Gavin, B.A., S.E. Arruda, and P.J. Dolph. 2007. The role of carcineine in signaling at the *Drosophila* photoreceptor synapse. *PLoS Genet.* 3:e206. <http://dx.doi.org/10.1371/journal.pgen.0030206>

Gong, W.J., and K.G. Golic. 2003. Ends-out, or replacement, gene targeting in *Drosophila*. *Proc. Natl. Acad. Sci. USA*. 100:2556–2561. <http://dx.doi.org/10.1073/pnas.0535280100>

Gonzalez, M., S. Nampoothiri, C. Kornblum, A.C. Oteyza, J. Walter, I. Konidari, W. Hulme, F. Speziani, L. Schöls, S. Züchner, and R. Schüle. 2013. Mutations in phospholipase DDHD2 cause autosomal recessive hereditary spastic paraparesis (SPG54). *Eur. J. Hum. Genet.* 21:1214–1218. <http://dx.doi.org/10.1038/ejhg.2013.29>

Hart, A.C., H. Krämer, D.L. Van Vactor Jr., M. Paidhungat, and S.L. Zipursky. 1990. Induction of cell fate in the *Drosophila* retina: the bride of sevenless protein is predicted to contain a large extracellular domain and seven transmembrane segments. *Genes Dev.* 4:1835–1847. <http://dx.doi.org/10.1101/gad.4.11.1835>

Higgs, H.N., and J.A. Glomset. 1996. Purification and properties of a phosphatidic acid-prefering phospholipase A1 from bovine testis. Examination of the molecular basis of its activation. *J. Biol. Chem.* 271:10874–10883. <http://dx.doi.org/10.1074/jbc.271.18.10874>

Huber, A., D.P. Smith, C.S. Zuker, and R. Paulsen. 1990. Opsin of Calliphora peripheral photoreceptors R1-6. Homology with *Drosophila* Rh1 and post-translational processing. *J. Biol. Chem.* 265:17906–17910.

Katanosaka, K., F. Tokunaga, S. Kawamura, and K. Ozaki. 1998. N-linked glycosylation of *Drosophila* rhodopsin occurs exclusively in the amino-terminal domain and functions in rhodopsin maturation. *FEBS Lett.* 424:149–154. [http://dx.doi.org/10.1016/S0014-5793\(98\)00160-4](http://dx.doi.org/10.1016/S0014-5793(98)00160-4)

Klumperman, J. 2000. Transport between ER and Golgi. *Curr. Opin. Cell Biol.* 12:445–449. [http://dx.doi.org/10.1016/S0955-0674\(00\)00115-0](http://dx.doi.org/10.1016/S0955-0674(00)00115-0)

Kohyama-Koganeya, A., Y.J. Kim, M. Miura, and Y. Hirabayashi. 2008. A *Drosophila* orphan G protein-coupled receptor BOSS functions as a glucose-responding receptor: loss of boss causes abnormal energy metabolism. *Proc. Natl. Acad. Sci. USA.* 105:15328–15333. <http://dx.doi.org/10.1073/pnas.0807833105>

Kondylis, V., H.E. van Nispen tot Pannerden, B. Herpers, F. Friggi-Grelin, and C. Rabouille. 2007. The golgi comprises a paired stack that is separated at G2 by modulation of the actin cytoskeleton through Abi and Scar/WAVE. *Dev. Cell.* 12:901–915. <http://dx.doi.org/10.1016/j.devcel.2007.03.008>

Küster, B., S.F. Wheeler, A.P. Hunter, R.A. Dwek, and D.J. Harvey. 1997. Sequencing of N-linked oligosaccharides directly from protein gels: in-gel deglycosylation followed by matrix-assisted laser desorption/ionization mass spectrometry and normal-phase high-performance liquid chromatography. *Anal. Biochem.* 250:82–101. <http://dx.doi.org/10.1006/abio.1997.2199>

Li, H.S., and C. Montell. 2000. TRP and the PDZ protein, INAD, form the core complex required for retention of the signalplex in *Drosophila* photoreceptor cells. *J. Cell Biol.* 150:1411–1422. <http://dx.doi.org/10.1083/jcb.150.6.1411>

Lowe, M.E. 1992. The catalytic site residues and interfacial binding of human pancreatic lipase. *J. Biol. Chem.* 267:17069–17073.

Maley, F., R.B. Trimble, A.L. Tarentino, and T.H. Plummer Jr. 1989. Characterization of glycoproteins and their associated oligosaccharides through the use of endoglycosidases. *Anal. Biochem.* 180:195–204. [http://dx.doi.org/10.1016/0003-2697\(89\)90115-2](http://dx.doi.org/10.1016/0003-2697(89)90115-2)

Nakajima, K., H. Sonoda, T. Mizoguchi, J. Aoki, H. Arai, M. Nagahama, M. Tagaya, and K. Tani. 2002. A novel phospholipase A1 with sequence homology to a mammalian Sec23p-interacting protein, p125. *J. Biol. Chem.* 277:11329–11335. <http://dx.doi.org/10.1074/jbc.M111092200>

Ong, Y.S., B.L. Tang, L.S. Loo, and W. Hong. 2010. p125A exists as part of the mammalian Sec13/Sec31 COPII subcomplex to facilitate ER–Golgi transport. *J. Cell Biol.* 190:331–345. <http://dx.doi.org/10.1083/jcb.201003005>

Pathre, P., K. Shome, A. Blumenthal-Perry, A. Bielli, C.J. Haney, S. Alber, S.C. Watkins, G. Romero, and M. Aridor. 2003. Activation of phospholipase D by the small GTPase Sar1p is required to support COPII assembly and ER export. *EMBO J.* 22:4059–4069. <http://dx.doi.org/10.1093/emboj/cgd390>

Pelham, H.R. 1989. Control of protein exit from the endoplasmic reticulum. *Annu. Rev. Cell Biol.* 5:1–23. <http://dx.doi.org/10.1146/annurev.cb.05.110189.000245>

Pfeffer, S.R., and J.E. Rothman. 1987. Biosynthetic protein transport and sorting by the endoplasmic reticulum and Golgi. *Annu. Rev. Biochem.* 56:829–852. <http://dx.doi.org/10.1146/annurev.bi.56.070187.004145>

Rademacher, T.W., R.B. Parekh, and R.A. Dwek. 1988. Glycobiology. *Annu. Rev. Biochem.* 57:785–838. <http://dx.doi.org/10.1146/annurev.bi.57.070188.000433>

Rao, R.P., C. Yuan, J.C. Allegood, S.S. Rawat, M.B. Edwards, X. Wang, A.H. Merrill Jr., U. Acharya, and J.K. Acharya. 2007. Ceramide transfer protein function is essential for normal oxidative stress response and lifespan. *Proc. Natl. Acad. Sci. USA.* 104:11364–11369. <http://dx.doi.org/10.1073/pnas.0705049104>

Rothman, J.E. 1994. Mechanisms of intracellular protein transport. *Nature.* 372:55–63. <http://dx.doi.org/10.1038/372055a0>

Saito, K., M. Chen, F. Bard, S. Chen, H. Zhou, D. Woodley, R. Polischuk, R. Schekman, and V. Malhotra. 2009. TANGO1 facilitates cargo loading at endoplasmic reticulum exit sites. *Cell.* 136:891–902. <http://dx.doi.org/10.1016/j.cell.2008.12.025>

Sato, S., H. Inoue, T. Kogure, M. Tagaya, and K. Tani. 2010. Golgi-localized KIAA0725p regulates membrane trafficking from the Golgi apparatus to the plasma membrane in mammalian cells. *FEBS Lett.* 584:4389–4395. <http://dx.doi.org/10.1016/j.febslet.2010.09.047>

Schuurs-Hoeijmakers, J.H., M.T. Geraghty, E.J. Kamsteeg, S. Ben-Salem, S.T. de Bot, B. Nijhof, I.I. van de Vondervoort, M. van der Graaf, A.C. Nobau, I. Otte-Höller, et al. FORGE Canada Consortium. 2012. Mutations in DDHD2, encoding an intracellular phospholipase A(1), cause a recessive form of complex hereditary spastic paraparesia. *Am. J. Hum. Genet.* 91:1073–1081. <http://dx.doi.org/10.1016/j.ajhg.2012.10.017>

Shimoi, W., I. Ezawa, K. Nakamoto, S. Uesaki, G. Gabreski, M. Aridor, A. Yamamoto, M. Nagahama, M. Tagaya, and K. Tani. 2005. p125 is localized in endoplasmic reticulum exit sites and involved in their organization. *J. Biol. Chem.* 280:10141–10148. <http://dx.doi.org/10.1074/jbc.M409673200>

Sisson, J.C., C. Field, R. Ventura, A. Royou, and W. Sullivan. 2000. Lava lamp, a novel peripheral golgi protein, is required for *Drosophila melanogaster* cellularization. *J. Cell Biol.* 151:905–918. <http://dx.doi.org/10.1083/jcb.151.4.905>

Tani, K., T. Mizoguchi, A. Iwamatsu, K. Hatsuzawa, and M. Tagaya. 1999. p125 is a novel mammalian Sec23p-interacting protein with structural similarity to phospholipid-modifying proteins. *J. Biol. Chem.* 274:20505–20512. <http://dx.doi.org/10.1074/jbc.274.29.20505>

Tesson, C., M. Nawara, M.A. Salih, R. Rossignol, M.S. Zaki, M. Al Balwi, R. Schule, C. Mignot, E. Obre, A. Bouhouche, et al. 2012. Alteration of fatty-acid-metabolizing enzymes affects mitochondrial form and function in hereditary spastic paraparesia. *Am. J. Hum. Genet.* 91:1051–1064. <http://dx.doi.org/10.1016/j.ajhg.2012.11.001>

Tsunoda, S., J. Sierralta, Y. Sun, R. Bodner, E. Suzuki, A. Becker, M. Socolich, and C.S. Zuker. 1997. A multivalent PDZ-domain protein assembles signalling complexes in a G-protein-coupled cascade. *Nature.* 388:243–249. <http://dx.doi.org/10.1038/40805>

Venken, K.J., Y. He, R.A. Hoskins, and H.J. Bellen. 2006. P[acman]: a BAC transgenic platform for targeted insertion of large DNA fragments in *D. melanogaster*. *Science.* 314:1747–1751. <http://dx.doi.org/10.1126/science.1134426>

Walther, R.F., and F. Pichaud. 2006. Immunofluorescent staining and imaging of the pupal and adult *Drosophila* visual system. *Nat. Protoc.* 1:2635–2642. <http://dx.doi.org/10.1038/nprot.2006.379>

Warming, S., N. Costantino, D.L. Court, N.A. Jenkins, and N.G. Copeland. 2005. Simple and highly efficient BAC recombineering using galK selection. *Nucleic Acids Res.* 33:e36. <http://dx.doi.org/10.1093/nar/gni035>

Webel, R., I. Menon, J.E. O'Tousa, and N.J. Colley. 2000. Role of asparagine-linked oligosaccharides in rhodopsin maturation and association with its molecular chaperone, NinaA. *J. Biol. Chem.* 275:24752–24759. <http://dx.doi.org/10.1074/jbc.M002668200>

Wernet, M.F., T. Labhart, F. Baumann, E.O. Mazzoni, F. Pichaud, and C. Desplan. 2003. Homothorax switches function of *Drosophila* photoreceptors from color to polarized light sensors. *Cell.* 115:267–279. [http://dx.doi.org/10.1016/S0092-8674\(03\)00848-1](http://dx.doi.org/10.1016/S0092-8674(03)00848-1)

Wheatley, M., and S.R. Hawtin. 1999. Glycosylation of G-protein-coupled receptors for hormones central to normal reproductive functioning: its occurrence and role. *Hum. Reprod. Update.* 5:356–364. <http://dx.doi.org/10.1093/humupd/5.4.356>

Zanetti, G., K.B. Pahuja, S. Studer, S. Shim, and R. Schekman. 2012. COPII and the regulation of protein sorting in mammals. *Nat. Cell Biol.* 14:20–28. <http://dx.doi.org/10.1038/ncb2390>

